CIAMTIS

U.S. DOT Region 3 University Transportation Center

Bridge Weigh in Motion For Simultaneous Multiple Vehicles

April 28, 2022

Prepared by:

R. Sarlo, A. Moghadam, Virginia Tech

r3utc.psu.edu

PennState College of Engineering

LARSON TRANSPORTATION INSTITUTE

DISCLAIMER

Technical Report Documentation Page

1. Report No.	2. Government Accession No.	3. Recipient's Catalog No.
CIAM-UTC-REG27		

4. Title and Subtitle	5. Report Date
Bridge Weigh in Motion for Simultaneous Multiple Vechicles	May 19, 2022
	6. Performing Organization Code

7. Author(s)	8. Performing Organization Report No.
Rodrigo Sarlo, Amin Moghadam	

9. Performing Organization Name and Address	10. Work Unit No. (TRAIS)
Virginia Tech Department of Civil and Environmental Engineering 200 Patton Hall, 750 Drillfield Dr. Blacksburg, VA 24060	**11. Contract or Grant No.**69A3551847103

12. Sponsoring Agency Name and Address	13. Type of Report and Period Covered
U.S. Department of Transportation Research and Innovative Technology Administration 3rd Fl, East Bldg E33-461 1200 New Jersey Ave, SE Washington, DC 20590	01/20/2020 – 05/20/2022
	14. Sponsoring Agency Code

15. Supplementary Notes

Eric Donnell, etd104@psu.edu ; Steven Williams, smw5@psu.edu, 814-863-5621

16. Abstract

Civil highway infrastructure is susceptible to deterioration caused by aging, harsh weather conditions, and natural hazards. Also, the rapid growth of traffic volume, particularly vehicle overweight enforcement, on degraded bridges increases the safety concerns and maintenance challenges for transportation agencies. These factors can adversely affect the bridges and highways' pavement condition and safety and cause serious issues to them such as fatigue, cracks, or even collapse. Intelligent Traffic Systems (ITS) and Structural Health Monitoring (SHM) have the potential to save highway infrastructure managers millions in traffic control and maintenance operations, respectively. The integration of the two systems is more attractive to practitioners because it brings improved value. That is, on one hand, ITS can make SHM estimates more accurate by providing load information. On the other hand, SHM can complement ITS data to help assess the impact of traffic on bridge condition. By fusing system information, less sensors may be required overall. Thus, an integrated, cost-effective monitoring system can be beneficial for the transportation agencies to first, detect the overloaded vehicles without disrupting the traffic, and second, regularly monitor the bridge integrity without imposing much additional cost. This study demonstrates the value of the fusion of SHM and ITS data for global bridge asset management using a high fidelity finite element model of a concrete box girder bridge and various combinations of traffic patterns and bridge damages.

17. Key Words	18. Distribution Statement
Intelligent Traffic System, Weigh in Motion, Structrual Health Monitoring	No restrictions. This document is available from the National Technical Information Service, Springfield, VA 22161

19. Security Classif. (of this report)	20. Security Classif. (of this page)	21. No. of Pages	22. Price
Unclassified	Unclassified	49	

Table of Contents

List of Figures

List of Tables

CHAPTER 1

Introduction

BACKGROUND

Civil highway infrastructure is susceptible to deterioration caused by aging, harsh weather conditions, and natural hazards [1]. Also, the rapid growth of traffic volume, particularly vehicle overweight enforcement, on degraded bridges increases the safety concerns and maintenance challenges for transportation agencies [2]. These factors can adversely affect the bridges and highways' pavement condition and safety and cause serious issues to them such as fatigue, cracks, or even collapse [3], [4].

Intelligent Traffic Systems (ITS) and Structural Health Monitoring (SHM) have the potential to save highway infrastructure managers millions in traffic control and maintenance operations, respectively. However, implementation of these systems individually by industry has been slow [5]. The integration of the two systems is more attractive to practitioners because it brings improved performance at a lower cost. That is, on one hand, ITS can make SHM estimates more accurate by providing load information. On the other hand, SHM can complement ITS data to help assess the impact of traffic on bridge condition. By fusing system information, less sensors may be required overall. Thus, an integrated, cost-effective monitoring system can be beneficial for the transportation agencies to first, detect the overloaded vehicles without disrupting the traffic, and second, regularly monitor the bridge integrity without imposing much additional cost. This study demonstrates the value of the fusion of SHM and ITS data for global bridge asset management where traffic data can be used to more precisely quantify traffic loading history on bridges, aiding in the overall asset management of these structures.

1.1. ITS and Traffic Monitoring

In the context of detecting traffic patterns and overloaded trucks, pavement-based weigh-in-motion (WIM) systems [6]–[8] are already in use to provide valuable information for traffic monitoring and weight enforcement [9]. However, pavement-based WIM systems use devices such as load cells, capacitance mats, bending plates, and etc., which must be embedded in the pavement. This causes some issues such as labor intensity as well as sensors durability problem and long-term maintenance costs as they are exposed to daily tire impacts and harsh weather condition [10]. Also, lane closures are required during installation and maintenance operations, resulting in additional costs and traffic disruption.

In contrast, bridge-weigh-in-motion (BWIM), first introduced by Moses [11], is a less intrusive solution which uses the bridge as a scale for weight estimation. This system is usually undetectable by drivers, and easier to install. In Moses' approach, the truck speed, the number of axles, and the axles spacing should be obtained in advance. These parameters are called "Prerequisites" in this study. For prerequisite estimation, several BWIM types are proposed in the literature, including traditional BWIM [12], contactless BWIM (cBWIM) [13], [14], and Nothing-on-Road (NOR) BWIM [15]–[18]. However, this study focuses on NOR BWIM systems due to its inherent advantages. In this system, unlike other categories, all devices are easily installed under the bridge and nothing is on the road surface; thus, this extends the durability of the monitoring system as they are not exposed to daily tire impacts and harsh weather condition. Furthermore, no traffic control or lane closure is needed during installation and maintenance, reducing installation and maintenance costs. Additionally, regular strain gauges are the most

common sensors used in this system and no additional sensors such as Free-of-Axle (FAD) detectors [19], switch tapes, pneumatic tubes, etc. are needed. On the one hand, this provides the possibility of using existing sensors for SHM applications and, on the other hand, makes the system even more affordable compared to other BWIM systems and pavement-based WIMs due to the sensors' cost itself [8], [9]. Recent NOR BWIM techniques and their drawbacks are discussed in Subsection 1.1.1. Once the Prerequisite are obtained, they will be used for weight estimation. The weight estimation techniques are discussed in Subsection 1.1.2.

1.1.1. BWIM prerequisites estimation techniques

Prerequisites estimation requires the time delay between the peaks in the strain response caused by traversing axles over the bridge. However, peak clarity/sharpness in the response depends on two main factors. First, the bridge construction method, which changes the global behavior of the bridge and load-transfer mechanism from the slab to other bridge components when the truck gets close to the sensors. Second, the properties of slab itself (such as slab stiffness and thickness), which influence the local strain right under the tire path due to a concentrated load; thus, right sensor placement which captures most of the local strains at the vicinity of the tires' concentrated loads can improve peak sharpness, particularly for closely spaced axles. Many studies obtained this information directly from the raw strain response measurements [17], [18], [20], [21]. However, there are some cases in which the peaks are not clearly observable in the recorded responses. Thus, they have proposed particular processing methods which result more observable and sharper peaks [22]–[25]. These techniques are either signal-processing-based or physics-based. In signal-processing-based techniques, tools such as continuous wavelet transform (CWT) are used [23] for feature generation; however, in physics-based techniques, either the internal forces (shear [24], moments [22]}, etc.) at certain points in the bridge and their combination are used or the truck axles' weights [25], [26]. An example for the latter case is the virtual axle method [25], in which the truck was initially assumed to have a large number of evenly distributed virtual axles. Then, using Moses's algorithm, the weights of all axles were obtained to find the virtual/true axles knowing that the virtual axles have zero weights.

However, these methods only tested on T-beam bridges while other bridge types may reveal a different strain profile where the number of axles and their positions are directly observable from the response such that no further methods are needed to be involved. Thus, other bridge types should be evaluated, particularly long-spans where significant dynamic effects induced by vehicles may affect the difficulty of the process and accuracy. Also, in all these studies, the techniques were evaluated either using numerical or/and prototype models in lab which are not usually representative of real conditions.

1.1.2. BWIM weight estimation techniques

Once the prerequisites are obtained, they are used for weight estimation. In general, weight estimation methods can be classified into two different groups: 1) dynamic methods [24], [27]–[30] and 2) static methods [31]–[34]. However, in dynamic methods, for a satisfactory accuracy, a full 3D model is usually needed. This makes the computation very time-consuming such that it will not be suitable for real-time monitoring applications [35]. In contrast, static methods directly deal with measured data and no model is needed, and this makes the static methods adequate for real-time monitoring applications. In the static methods, the influence line is the main requirement for weighing the trucks in motion on bridges [36]. This will be computed through a procedure known as "calibration" by minimizing the difference between the theoretical and measured responses. There are some studies in which the influence line is experimentally obtained using crossing vehicles with known weight and strain responses. In this regard, in 2006, a novel method was proposed using strain measurements from a single passage of a single calibration truck [37]. In 2009, Tikhonov regularization was used to improve the accuracy of the Moses's algorithm [38]. In 2015, Maximum Likelihood Estimation (MLE) method was introduced taking the

measurements from multiple calibration trucks for influence line estimation [39]. Then, in 2018, the concept of probabilistic influence line seeking was introduced for the most probable axle weights extraction [33]. However, in 2019, in a comparative study, it was shown that MLE method provides the most accurate results [40], and this is why MLE method is the focus of this study for weight estimation.

The main limitation with both studies on prerequisites and weight estimations is their short span-length while long-spans may show different behavior. The common wisdom [19], [41] in the literature is that short-span or medium-span bridges and the ones with secondary elements, such as orthotropic bridges, are the best choices for NOR-BWIM system. The first reason is the simplicity of the data analysis since long-spans are more likely to combine the peaks created by closely spaced axles and to demonstrate only their combined contributions [41]. This can be due to the fact that longer-spans are usually deeper, and such elements (such as thicker top slab) will usually provide less sharp peaks. The second reason in the literature is that longer-span bridges have lower natural frequencies that are more likely to match the vehicle frequencies increasing the dynamics effect [10]. Thus, like the studies discussed above, most of the NOR-BWIM applications in the literature have focused on either short-spans (span-length < 30m) [24], [42], [43]. Thus, the longer-span bridges should be considered further because of several reasons. Firstly, deeper elements, such as thicker top slabs, may still provide sharp peaks for prerequisite estimation depending on construction and sensor placement. Secondly, for bridges with relatively smooth road surfaces, the level of error due to dynamics effects can be still in a reasonable range and one may actually be able to still use the long-spans for NOR-BWIM as well. Thirdly, there are many long-span bridges throughout the world which are highly instrumented to be evaluated from the structural integrity point of view. Thus, the existing sensors for structural health monitoring (SHM) system can be used to integrate the SHM systems with NOR-BWIM systems to reduce the cost. Hence, further evaluation is needed for the long-spans to understand how the accuracy of the results is and whether or not they can be chosen for NOR-BWIM systems at all.

Also, when multiple trucks are simultaneously on the bridge, the standard BWIM methods are not able to properly decompose the strain responses associated with each truck. This causes overestimation of the trucks' weights. There are only limited studies about multiple-truck presence. Current methods still require either time consuming IL calibration [44] or are applicable to a small set of possible traffic combinations [45]. The concept of influence surface instead of influence line was introduced for multiple-truck presence by Quilligan et al. [44] and was later used for other applications such as transverse position and others [46], [47]. However, in the influence surface calibration procedure, series of transverse positions should be considered to cover all possible truck positions within two traffic lanes [48]. This makes it time-consuming and thus, less applicable for commercial applications. Also, during influence surface calibration, there should not be unwanted vehicles on the bridge. This can only be possible for short-span bridges with limited traffic volume. Additionally, it is computationally demanding since the system expands in both the number of equations and in complexity, and thus, linear methods cannot usually be used [48]. These disadvantages can become worse for bridges with multiple lanes in each direction.

In another study, a weight estimation procedure was proposed using a load distribution factor and considering how the truck weight is distributed between different lanes when it travels in a particular lane and on slab-on-girder bridges [45]. This was verified against a series of indoor experiments on only slab-on-girder bridges, showing that the method could work under the presence of only two vehicles in one row. Side-by-side and more complex traffic patterns were ignored. However, this can be a limitation for bridges with multiple lanes and dense traffic and leads to the selection of short-span bridges. For a multiple-lane bridge with a large amount of traffic, the presence of multiple trucks combined with light-weight vehicles, arbitrarily distributed in different lanes, is very common. This is the topic of Phase I of this study explained in Section 1.3.

1.2. Bridge health monitoring

With respect to SHM, two main families have been suggested by researchers in the past few decades for the global SHM methods [49]. The first one consists of the methods established based on either the structural dynamic properties such as natural frequencies, damping ratios, and mode shapes [50], [51], or related characteristics (e.g., modal assurance criterion, modal strain energy, etc.) [52]–[55]. These methods have illustrated varying degrees of success in the previous studies. However, they are usually insensitive to local damages in large-scale structures (such as bridges) and sensitive to environmental effects [49].

The second SHM family is based on the static properties of the structures. In this study, the unite influence line (UIL) method is selected due to its inherent potentiality for BWIM systems' adjustment and great capability in SHM applications (discussed later in this section). The first step in vehicle information computation using BWIM is always influence line (IL) calculation using experimental data. Furthermore, suppose the stiffness of the indeterminate bridge changes due to damage at a certain point. In that case, the structural response and, consequently, the IL of the bridge will change due to internal force redistribution. This concept can be used for bridge integrity monitoring applications. Thus, IL can be a connecting element to convert the SHM and BWIM systems to a single, multi-functional system. In fact, besides BWIM's excellent capability in weight enforcement estimation, it can also be appropriately adjusted for structural health monitoring (SHM) using the existing sensors and the bridge IL.

Bridge monitoring using IL calculation can circulate around different structural quantities. These include displacement influence line [56]–[58], rotation influence line [4], [59], strain/stress influence line [26], [49], [60]. However, this study aims to integrate the BWIM and SHM systems. In most cases, the BWIM system relies on strain measurements due to applicability to different types of bridges and simplicity in measurement and prerequisites calculation.

In this regard (stress/strain IL in SHM), in some cases, IL was indirectly used for SHM (usually BWIM-informed SHM systems). For instance, a WIM-based method was proposed along with a damage index for level I damage detection [60]. Two types of WIM systems were used, pavement-based and BWIM. IL was employed for the BWIM weight estimation. The ratio of the computed weights using these two systems was used as a damage index. This was based on the fact that the truck weight computed using BWIM on the damaged bridge will be different from the weight computed on the intact bridge. In another study, called the “virtual axle” method, an additional weightless axle was assumed for the traversing vehicle to detect damage [60]. It was shown that any change in structural behavior caused by damage would lead to a non-zero estimate for the virtual axle. This was used as a damage indicator.

In a more direct application of stress IL in SHM, a regularization method was proposed for the stress influence line based on a train passing over Tsing Ma Bridge in Hong Kong [49]. Three damage indexes were introduced and tested, including the IL change and its corresponding first-order and second-order differences, showing satisfying results.

However, these studies have two significant shortcomings. 1) They are only applicable when a single truck is on the bridge. In fact, when multiple trucks are simultaneously on the bridge, these IL methods cannot properly decompose the strain responses associated with each truck. Thus, since it is not guaranteed to only have one truck on the bridge at the monitoring stage without the lane closure, they are not practical for long and medium-span bridges. 2) Two challenging factors, i.e., noise and transverse positions, are ignored while these can make a false damage indicator even for the intact bridge and need to be included in the process.

1.3. Research phases and objectives

1.3.1. Phase I

To demonstrate the feasibility and limitations of the ITS studies discussed in Section 1.1 for both prerequisites and weight estimation in a new experimental context, a different but common type of bridge, a concrete-box-girder, was considered. The construction method in this type of bridge makes the slab and webs integrated. As discussed earlier, this results in a different load-transfer mechanism from the spanning slabs to the webs compared to other bridge types. It was aimed to demonstrate a low-cost, NOR-BWIM system for long-span, concrete-box-girders and evaluating the accuracy of the results to understand if NOR-BWIM systems (for prerequisite estimation) and MLE method (for weight estimation) are still suitable for this particular bridge.

The main advantage of the proposed approach is that it successfully decomposes the strain responses of each vehicle in multiple-vehicle cases, with a combination of heavy and light-weight vehicles simultaneously on the bridge. The idea behind the approach is that it removes the non-localized portion of the strain response (later explained further), keeping only the localized peaks which are not sensitive to nearby loads. This approach only needs a single strain gauge per lane for weight estimation, thus making the system affordable significantly. This approach can also be used for more advanced BWIM systems such as NOR-BWIM.

Another main advantage of this approach is that even if the calibration truck (with known prerequisites) is surrounded by unwanted vehicles, unlike standard BWIM techniques discussed above, no lane-closure is needed for IL calibration, and the proposed approach can be used to successfully decompose the strain response associated with the calibration truck. This makes the system more cost-effective and safer and, as a result, more commercially feasible.

To show the feasibility of the approach, the Varina-Enon Bridge, a long-span bridge with three lanes in each direction, was considered. Then, a finite element (FE) model of the bridge was made and validated against the experimental data (strain-time response) under known large events. In general, in heavy-traffic bridges, it is very difficult to control the traffic. Thus, the FE model was used to consider single-truck events (for proof-of-concept) as well as complex multiple-truck traffic cases, including in-one-row trucks, zigzag patterns, side-by-side trucks, and a combination of several trucks with several light-weight vehicles involved.

1.3.2. Phase II

To address these shortcomings discussed in Section 1.2, this study proposes a dual-purpose structural health monitoring (SHM) approach. This is to simultaneously monitor the integrity of multiple bridges (level I damage detection) located between two physical points (e.g., within a state or city) using the existing sensors for BWIM systems. This procedure is called dual-purpose since it can be used for SHM and BWIM applications. The proposed procedure computes the change in the ILs of the bridges experimentally extracted at the regular monitoring stage compared to their initial ILs extracted from the intact bridges.

This procedure has three clear contributions to the literature: 1) for the first time in the literature, a novel IL extraction technique, called Multiple-Presence IL (MP-IL) in this study, is used for SHM application. MP-IL can successfully remove the effect of unwanted vehicles in complex multiple-truck traffic conditions and obtain the IL. This resolves the significant multiple-presence limitation of the standard BWIMs for IL extraction, weight estimation, and SHM. 2) Other important factors, such as noise and transverse position, are also considered in the proposed procedure to provide a more realistic bridge health monitoring approach. 3) An updated instrumentation plan is proposed to be effective for both the multiple-presence BWIM system and SHM in single-truck and multiple-truck events.

1.3.3 Deliverables

The deliverables of this work were as follows:

1) Create an experimentally validated finite element model (FEM) of the Varina Enon bridge for simulation of multiple truck presence scenarios as well as possible damage cases
2) Virtually test a novel technique for multiple-presence NOR-BWIM on long-span bridges.
3) Motivate the use of the technique as a complement for Structural Health Monitoring.

CHAPTER 2

Methodology

INTRODUCTION

This chapter covers the methodology for two phases discussed in Chapter 1: weight estimation in multiple-presence events, and dual-purpose SHM procedure.

2.1. Weight estimation in multiple-presence events

The weight estimation procedure has three steps. First, to calculate the prerequisites, i.e., number of axles, speed, and axle spacing. This is explained in Subsection 2.1.1. Second, influence line extraction (IL calibration) using known trucks with known prerequisites. Three, using the extracted influence line and the computed prerequisites for weight estimation of unknown traversing trucks.

In this section, for steps two and three, two approaches are provided. 1) standard BWIM approach (explained in Subsection 2.1.2) which can be used for only one truck on the bridge. 2) the proposed BWIM approach for multiple-truck presence (explained in Subsection 2.1.3) which can handle multiple trucks simultaneously on the bridge.

2.1.1. The Prerequisites' estimation approach

Prerequisites should be calculated using the physical distance between the successive sensors and the time delay between the peaks in the strain responses. The peaks are actually made due to a significant increase in the localized portion of the strains under the concentrated forces (axle weights). It is shown later in Chapter 4 that the strain response under a 5-axle truck passage, for instance, consists of five clear peaks when the sensors are placed in the right positions discussed in Chapter 3. This is equivalent to the number of traversing axles. In this study, the focus is weight estimation for multiple-truck cases, and it is assumed that the prerequisites were already computed properly. For further details on prerequisite computation, see two studies conducted by Deng et al. [24] and He et al. [22].

2.1.2. The Standard BWIM approach

The first step in the weight estimation procedure is the influence line extraction from calibration data. In general, there are some studies that experimentally compute the influence line [31], [33], [38], [39]. Additionally, according to a comparative study conducted by Carraro et al. [40], maximum likelihood estimation (MLE) is the most accurate method, and this is why the MLE method is the one used as the standard weight estimation approach.

MLE method was first proposed by Ieng [39]. This method takes multiple truck passages into account, considering the variability of the effects of the calibration vehicle on the bridge. Then, the extracted influence line will be used to estimate the weight of unknown trucks using the Moses method [11] shown in Equation 1. In Equation 1, W is a vector consisting of the unknown axles weights, and B is a matrix created using the influence line ordinates, shifted based on the truck axle spacings to adjust the

time-instant when each truck axle enters and leaves the bridge structure. Also, M is the measured strain vector.

$$W = (B^T B)^{-1} B^T M^m \quad \text{Equation (1)}$$

As mentioned earlier, standard BWIM approaches (including MLE) are not able to properly decompose the strain responses associated with each truck. This causes an overestimation of the trucks' weights. Thus, they can be used for only one truck on the bridge.

2.1.3. The multiple-presence (MP) NOR BWIM approach

The novel BWIM approach is proposed here to handle multiple-truck cases with arbitrary traffic

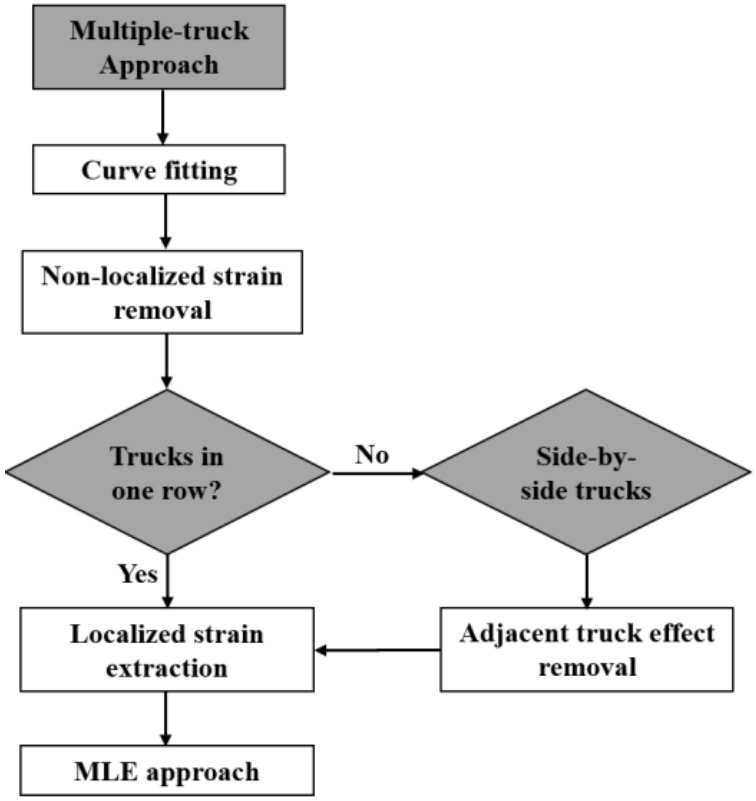

Figure 0.1. A flowchart for the proposed BWIM approach steps.

patterns, consisting of multiple trucks and light-weight vehicles involved. When the bridge is subjected to a truck load that is right on top of the sensors, the strain response under the truck tires consists of two components that should be superposed together: 1) the strain of the entire bridge span (acting as a beam) due to the internal moments which appears as slowly changing compression in the top slab and 2) additional strain due to the top plate/slab bending (plate behavior) which appears as sharp peaks in tension corresponding to axle crossings. These two strain portions are called localized and non-localized strains. As long as the load is not significant (such as traffic load) to make the material nonlinear, both terms will be linear and thus, BWIM theory can be used.

In this study, the proposed approach first properly decomposes the strain responses associated with each truck in multiple-truck strain responses. To do this, a curve should be fitted to the non-localized portion of the response (later explained in detail). The non-localized portion will be removed by subtracting the fitted carve from the original strain response. Then, the strain response associated with each truck will be extracted and fed into the standard BWIM procedure. In fact, the proposed approach has one additional step (strain decomposition) before the steps explained in the original studies for standard BWIM methods [40]. It should be noted that if there is any side-by-side truck, its effect should properly be removed (later explained in detail) before the strain response extraction for each truck. These steps are shown in Figure 2.1.

For one single-lane weight estimation, only one influence line is needed (similar to standard BWIM methods). However, for multiple-lane highways, multiple influence lines are needed (one for each). The advantage of this approach is that no lane closure is needed for IL calibration to ensure that only one truck is on the bridge during calibration. This is because even if the calibration truck (with known prerequisites) is surrounded by unwanted vehicles, the proposed approach can still be used to decompose the localized strain response associated with the calibration truck. Then, the decomposed strain responses will be used for influence line extraction, similar to standard BWIM methods.

Here, the decomposition procedure is explained. According to Figure 2.2.a (left side), a strain-time response extracted from a single-truck passage includes two portions: 1) localized portion under traversing axle weights, and 2) non-localized portion (dashed curve). The difficulties in processing strain-time responses for a multiple-truck case compared to a single-truck case are due mostly to distortions of the non-localized portion. In fact, a multiple-truck case will result in a deeper non-localized response than a single-truck case but with a similar localized strain portion. In the following, the proposed approach steps to decompose the strain responses under multiple trucks simultaneously on the bridge are explained.

In the first step to decompose the strain responses associated with each truck in a multiple-truck event, points P1 and P2, called ``critical points'' in Figure 2.2.a, should be calculated. These points should be selected approximately where the localized strain portion starts and ends. In this study, P1 and P2 were defined at 0.16 second before the first peak and 0.20 second after the last peak, respectively.

In the second step, a curve (dashed curve) should properly be fitted to the non-localized portion of the response. Then, the fitted curve should be subtracted from the original strain response to remove the non-localized portion to only keep the localized strain portion (modified response). This curve should meet a few requirements to provide satisfactory results: 1) for both single and multiple-truck cases, the curve should touch points P1 and P2 in Figure 2.2.a such that when the non-localized portion of the strain is removed, P1 and P2 will be equal to a number close to zero (less than about 0.3 microstrain, for instance), 2) the curve should be a lower convex envelope between P1 and P2 such that for multiple-truck cases, majority of lower peaks between P1 and P2 should also be touched).

An “envelope function” [61] can be used for this purpose. Envelope of a signal is a curve, smoothly connecting the maximum and minimums [61]. The outcome of an envelope function is two curves tangential to the input signal local minimums and maximums. However, only the lower envelope should be considered and the upper envelope should be discarded.

The envelope function can be used in any programming environment. In this study, it was found that the “Envelope” function in MATLAB can successfully satisfy these requirements when a proper “peak separation factor (np)” is selected. The envelopes are computed using spline interpolation over local minimums separated by at least np samples. The MATLAB code prepared for this study automatically checks different np values between 30-50 (found as the most effective range) and chooses the one that generates an envelope with smallest difference from P1. To do this, a loop was programmed that changes the np value in each step and chooses the one with the lowest generated P1 in the modified strain response (the non-localized response removed). It was observed that, through this procedure, the generated lower convex envelope curve between the critical points will be automatically generated and satisfies other requirements explained above. A flowchart is presented in Figure 2.3 to show these steps clearly.

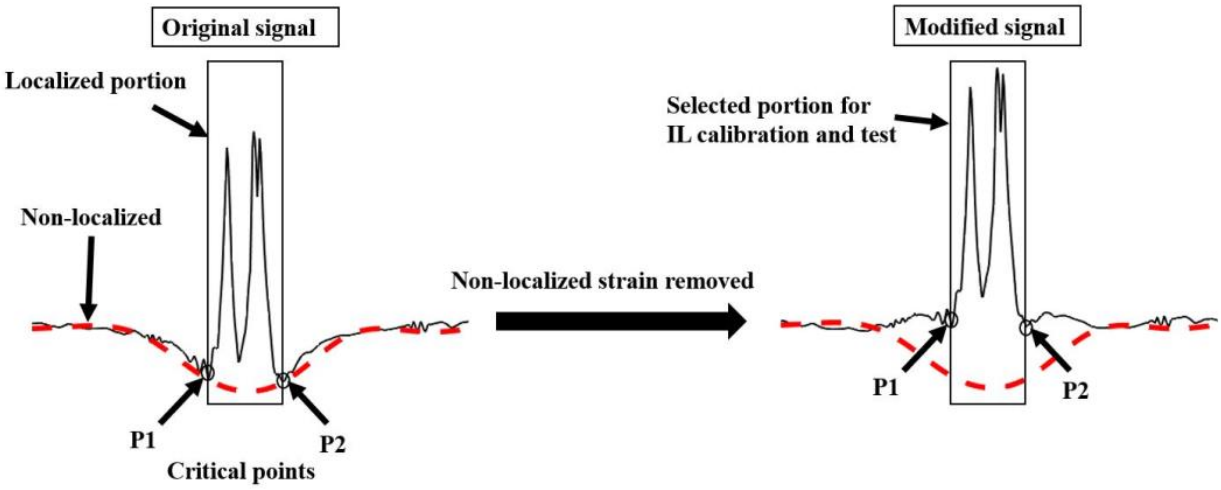

(a) Single-truck cases

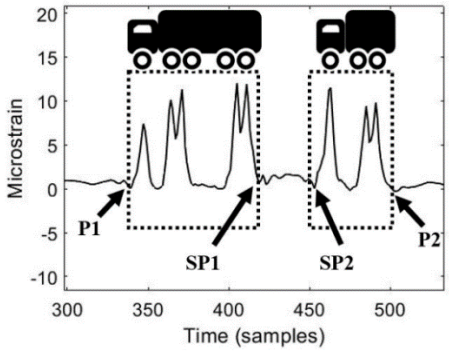

(b) In-one-row cases (non-localized strain removed)

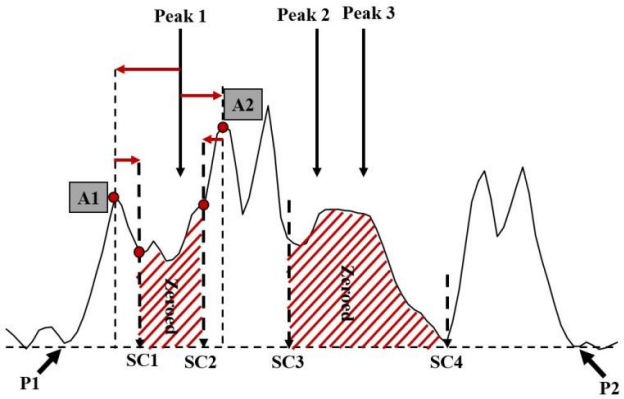

(c) Side-by-side cases (non-localized strain removed)

Figure 0.2. The proposed BWIM approach.

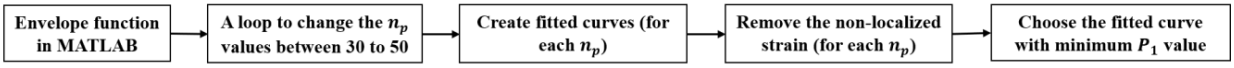

Figure 0.3. A flowchart for the best envelope fit.

It should be noted that other than the envelope function, two other techniques were also considered in this study while they did not work as properly as the envelope function technique to flatten the strain response (to remove the non-localized strain). These techniques included: 1) Manual fitting process that needs the user to manually build the curve in a trial and error process to find the best fit that generates P1 and P2 values close to zero when the non-localized response is removed. Thus, it can never be used for a

large number of events. Also, the accuracy of the results can differ depending on the user's accuracy. 2) High-pass filter with a small cut-off frequency selected based on the Fast Fourier Transform (FFT) of the strain response. However, it was found that the high-pass filter technique can flatten the strain response but distorts the localized portion of the response.

The third step is localized strain extraction. In this step, a small portion of the modified response, shown on the right side of Figure 2.2.a, should be selected to be used for IL calibration or test. For single-truck cases, this simply is the portion between P1 and P2 (already defined). However, the procedure is slightly different for multiple-truck cases. Multiple truck cases are either in one row, side-by-side, or a combination of these cases. For in-one-row multiple-truck cases (e.g., for a 5-axle and 3-axle truck shown in Figure 2.2.b, some secondary points, e.g., SP1 and SP2, should be selected in a way similar to the critical points. For instance, SP2 is located in 0.16 s before the first peak in the response associated with the 3-axle truck and SP1 is in 0.20 s after the last peak of the 5-axle truck. This procedure helps to decompose the strain responses for even closely moving trucks in one row. To know when a truck ends and the other starts in Figure 2.2.b, a proper threshold for the maximum axle spacing should be determined. When the distance between SP1 and SP2 exceeds from the threshold, the strain associated with the second truck starts. This threshold should statistically computed based on the traversing trucks (7 m in this study).

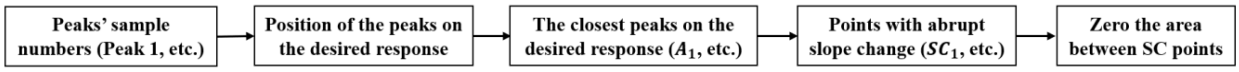

Figure 0.4. A flowchart for the adjacent truck effect removal.

For a case with two trucks moving side-by-side in two adjacent lanes, one additional step is needed between steps two and three explained above. This additional step is to remove the effect of the adjacent truck from the recorded strain-time response before feeding it into the proposed procedure. As it is later explained in Chapter 4, when a truck moves on a particular lane and the strain response is recorded on the same lane, sharp peaks will be obtained if a proper sensor placement, explained in Chapter 3, is employed. However, the strain response from the other lane will be distorted. This is clearly shown in Figure 2.2.c. This is the strain response for a 5-axle and 3-axle trucks moving side-by-side on lanes one and two, respectively, and the strain response is extracted from lane one. According to this figure, the strain response is a combination of clear and distorted peaks. However, only the clear peaks should be kept and the remaining should be properly removed for weight estimation.

To remove the adjacent truck effect, first the sample numbers of the peaks in the 3-axle truck strain response (from the second lane) should be manually obtained. Then, using the extracted sample numbers, the position of them should be found on the strain response extracted from the first lane. These are shown in Figure 2.2.c (Peak 1, Peak 2, and Peak 3). Then, these peak points (Peak 1, Peak 2, and Peak 3) should be used as a reference to find four other points (e.g., SC1, SC2, etc.), which show the area that should be removed. For instance, from Peak 1, one should move back and forward to find points A1 and A2, which are the closest peaks of the 5-axle truck in its strain response. Then, moving from points A1 and A2 on the 5-axle truck strain response towards Peak 1, SC1 SC2 will be obtained. These are where an abrupt change is made in the slope of the graph (>50%). The portion between these points should then be set to zero. The same procedure should be performed for Peaks 2 and 3 in Figure 2.2.c to find the second portion that should be zeroed (between SC3 and SC4). A flowchart is presented in Figure 2.4 to show these steps clearly. The reason why this area should be set to zero is that when one of the axles is right on top of the place where the strain response is extracted (for in-one-row events with no side-by-side trucks), a clear peak appears; however, immediately after that, the strain response goes to zero. Now that the adjacent truck effect (distorted responses) is removed, using the P1, P2 (already defined), the localized strain portion associated with the 5-axle truck should be selected. Other more complex traffic patterns.

e.g., zigzag, etc., can also follow the same steps explained for in-one-row and side-by-side cases as they are a combination of these two cases.

The fourth step is to feed the decomposed strain responses to MLE. All steps of the proposed approach are shown in Figure 2.1 for clarity. The IL extracted is called multiple-presence IL, or MP-IL, since can be extracted even in multiple-truck events.

As a last point in the methodology, it should be mentioned that another advantage of the proposed BWIM method compared to the standard BWIM method is its capability of dealing with variable speeds.

As explained above, the proposed method first decomposes the strains associated with each truck using the envelope function. This function is not dependent on the speed as it is just a mathematical operation.

Once the strains are decomposed, they will be used for weight estimation using the standard BWIM and Moses method. The assumption of standard BWIM is that the speed of each individual truck is constant when it passes over the weighing sensor. In the standard BWIM method, this takes 3-4 s or even longer (depending on the truck length and speed) since this method takes the entire strain response (both localized and non-localized portions of the response) into consideration, while for the proposed method it takes only 0.5-0.9 s as the method considers only the localized portion of the response. Thus, it is quite reasonable for the proposed method to say that the truck speed will remain constant in 0.5-0.9 s. This can be considered another advantage compared to the standard BWIM that considers a longer strain response where the truck speed is not guaranteed to remain constant.

2.2. Dual-purpose SHM approach

The novel influence line approach (MP-IL), explained in Subsection 2.1.3, handle multiple-truck events with a combination of heavy trucks and light-weight vehicles simultaneously on the bridge [62].

As explained earlier, MP-IL first filters out the non-localized strain portion (sensitive to nearby loads) and only keeps the localized portion. Then, the strain response corresponding to each truck should be properly extracted and fed into the standard IL approach such as MLE. The result will be called MP-IL.

This paper proposes a procedure to simultaneously monitor the integrity of multiple bridges (level I damage detection) located between two arbitrary points (within a city or state for instance) such as A and B (shown in Figure 2.5 using several known trucks with known configurations and weights. Many transportation agencies throughout the world need to regularly monitor the bridges' integrity, and this procedure addresses their need. The goal is to employ the existing sensors used for BWIM systems and, thus, to use the dual-purpose system for both BWIM and SHM applications. This makes the multi-functional system more affordable.

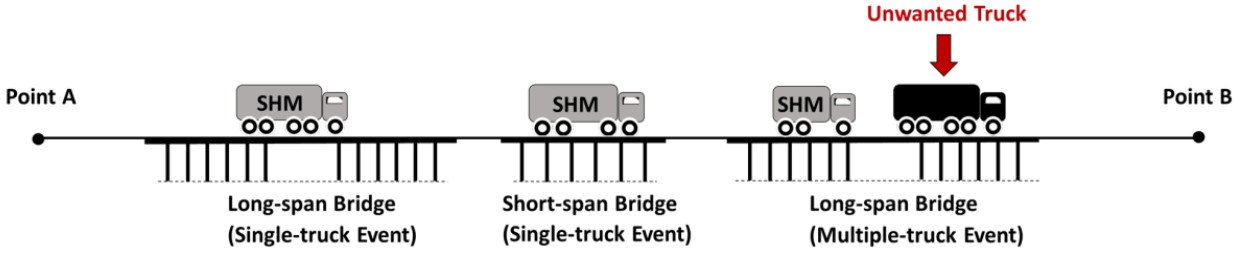

Figure 0.5. The cases occurred during bridge monitoring.

The proposed procedure circulates around the change in the ILs of the bridges (at the time of regular monitoring) compared to their initial/reference ILs extracted from the intact bridges. This procedure has two clear novelties. 1) for the first time in the literature, Multiple-Presence IL (MP-IL), is used for SHM application. MP-IL, unlike the standard IL extraction techniques, can successfully decompose the desired strain response associated with the corresponding truck to extract the IL of the bridge. MP-IL can also

remove the effect of the unwanted trucks simultaneously on the bridge. This resolves the significant multiple-presence limitation of the standard BWIMs for IL extraction, weight estimation, and SHM. 2) Other significant factors, i.e., noise and transverse position change, are included in the procedure to provide a more realistic and robust approach for SHM.

According to this procedure, to monitor the bridges (between points A and B shown in Figure 2.5, several SHM trucks with known but different axle configurations and weights will need to move from point A to point B separately and with a delay (e.g., 1 hour). When this happens, as shown in Figure 2.5, three cases may occur: 1) a single SHM truck on a long-span bridge, 2) a single SHM truck on a short-span bridge, and 3) multiple trucks (SHM truck surrounded by several unwanted trucks) on a long-span bridge. As mentioned earlier, IL change is the key to determine if any damage has occurred. Thus, for the first two cases (single-truck events), the standard IL technique should be used, but for the latter one (multiple-truck event) MP-IL should be employed for IL extraction. In both, the effects of noise and transverse position change are included. This is explained further later in this section.

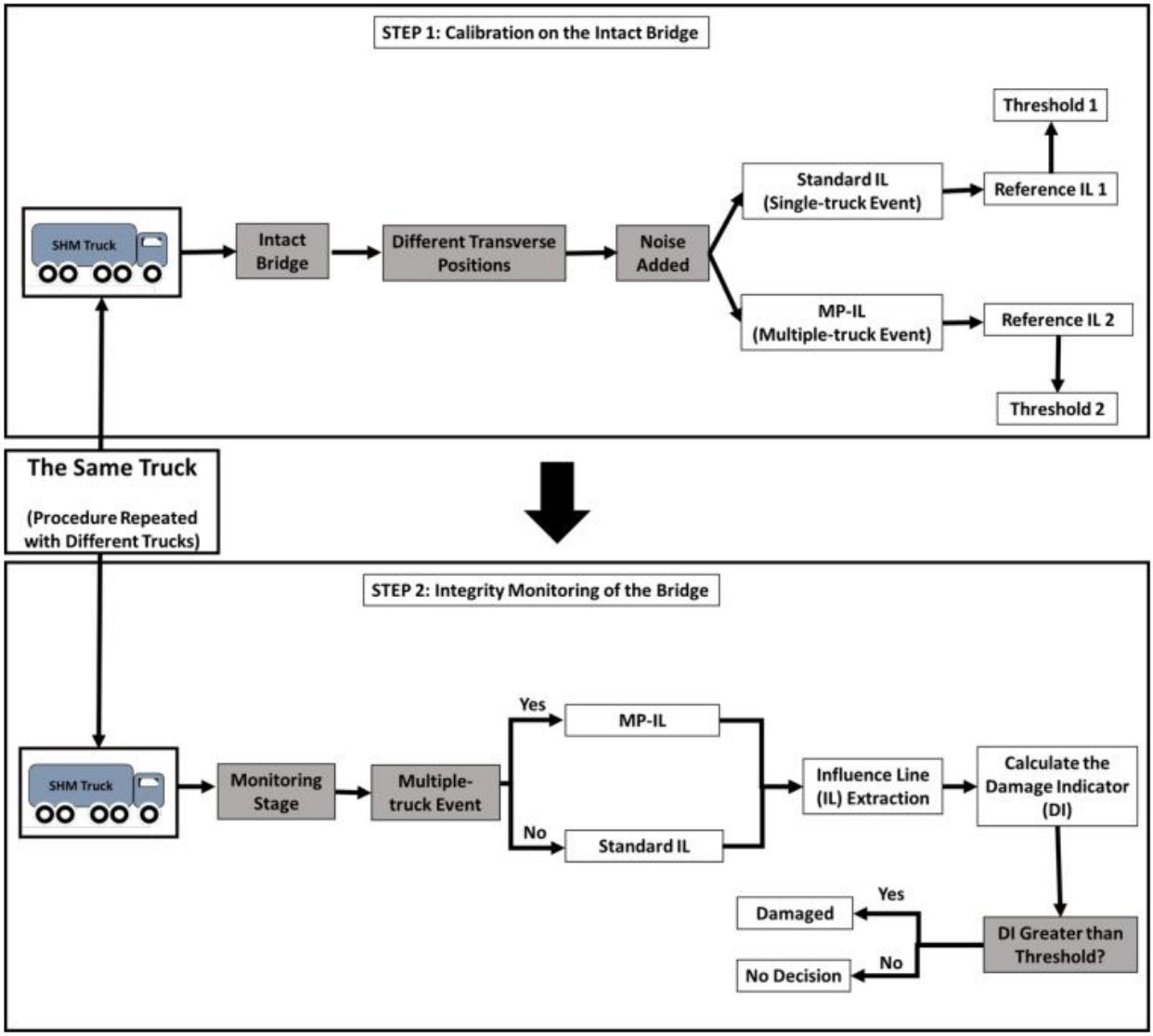

Figure 0.6. The dual-purpose SHM procedure.

In general, the dual-purpose procedure has two main steps shown in Figure 2.6. According to this figure, in the first step, i.e., "Calibration on the Intact Bridge", each SHM truck should move through each bridge, and the strain-time responses should be obtained. Then, the standard IL and MP-IL techniques will be applied to the responses to extract two ILs for each truck type. These ILs are the references for future bridge monitoring subjected to single-truck and multiple-truck events. Any change in ILs called "Damage Indicator (DI)" can be a sign of damage. DI will be the mean-square-error (MSE) of the reference IL and the IL at the monitoring stage. However, some factors, such as noise and transverse position, might still change the IL of the intact bridge. These factors, indeed, can create fake changes (fake damage indicator) to the IL of the intact bridge and thus, should be taken into consideration.

Thus, a significant amount of noise should be added to the responses from all variations of the truck transverse positions. Then, standard IL and MP-IL should be applied to the noisy responses for each truck in different transverse positions. Thus, for each truck, two reference ILs will be extracted, one using the standard IL method (for single-truck cases) and the other using MP-IL (for multiple-truck events) and will be used for future monitoring.

Once the reference ILs are extracted, two DI thresholds, one for single-truck cases and the other for multiple-truck cases (called thresholds 1 and 2, respectively), should be computed. The DI threshold is the 95% confidence analysis of the DIs calculated using the ILs extracted from intact bridges and on different transverse positions and subjected to different noise levels. Both thresholds 1 and 2 will be from the intact bridge but under single-truck events and multiple-truck events (SHM truck surrounded by unwanted trucks), respectively. These thresholds are to find a reliable range that can necessarily be related to a damage occurrence. If the DI value (at the monitoring stage) comes up to be greater than the thresholds, it can be concluded that damage has occurred with 95% confidence. If DI is smaller than that, we cannot necessarily conclude that damage has occurred even for a non-zero DI value.

The second step of the dual-purpose procedure, shown in Figure 2.6, is called "Integrity Monitoring of the Bridge". According to this figure, the same trucks with the same axle configurations and weights should again be used at the monitoring stage (every two years, for instance) to obtain the strain responses. Similar to the first step (Calibration on the Intact Bridge), for single-truck events and multiple-truck events, standard IL and MP-IL should respectively be used to obtain the ILs. Then, the DI will be the MSE of the new IL (at the monitoring stage) and the reference IL (for single-event, IL1, and for multiple-truck events, IL2). If the DI is greater than the DI thresholds, the bridge is damaged with 95% confidence. Otherwise, there is not enough evidence to decide about the integrity of the bridges.

CHAPTER 3

Analysis

INTRODUCTION

This section covers the finite element model and how it is validated against the experimental data (Subsection 3.1), the analysis procedure for MP NOR BWIM evaluation (Subsection 3.2), and the analysis approach for the proposed dual-purpose SHM procedure (Subsection 3.3).

3.1. Finite element model and experimental validation

3.1.1. Bridge Description

The Varina-Enon bridge (VEB), shown in Figure 3.1, is a cable-stayed, post-tensioned, concrete-box-girder bridge, along Interstate 295 and over the James River in Virginia with significant traffic flow. As shown in Figure 3.1.a, the total length of the bridge is 1426.5 m with twenty-eight spans. The main span (cable-stayed portion) consists of seven spans (13 to 19) with a total length of about 466 m. Furthermore, the south end of the bridge (left side in Figure 3.1.a) consists of two approach units (six 45.72-m spans each) while the north end (right side of the figure) includes two additional approach units, one with five and the other with four 45.72-m spans. Also, as shown in Figure 3.1.b (taken using a lidar scanner), there are eight external, post-tensioning tendons in each span of the approach units (four on the right side and four on the left side). Each tendon consists of nineteen 0.6-in-diameter strands.

According to Figure 3.1.c, the total width of the top slab is approximately 17.62 m, including three lanes (3.66 m each), and the two shoulders, which are 3.52 m and 3.12 m. The trapezoidal-shaped concrete box has a total height of about 3.66 m, with top and bottom slabs' depths of about 0.25 m (plus 5 cm topping) and 0.2 m, respectively. Figure 3.1.c shows the typical box dimensions for all spans; however, for two of the south spans (14 and 15) and two of the north spans (17 and 18), the boxes are tied together at each cable anchorage point by a delta frame. Since the focus of this study is span 6, the typical delta frame is not shown for conciseness.

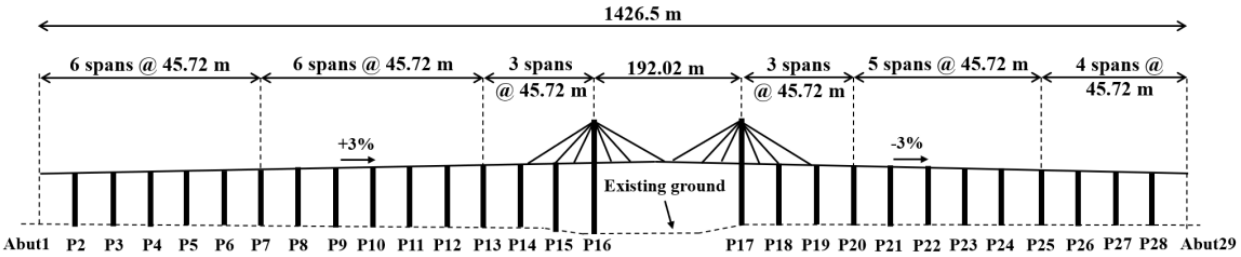

(a) The VEB side view.

Length (cm)	Width (cm)	Total bearing height (cm)	Total elastomer thickness (cm)	No. of elastomer layers	No. of Steel plates	Steel plates Thickness (mm)
91.4	91.4	13.5	11.4	10	9	1.6 (middle), 4.8 (other)

(b) The VEB inside view taken using a lidar scanner.

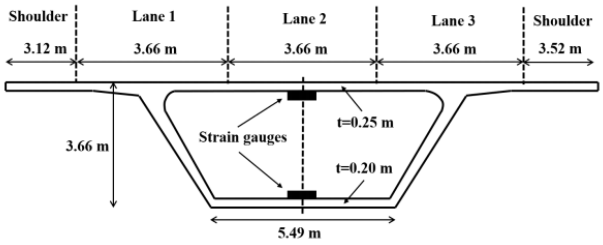

(c) The concrete box section and sensor position in the experimental validation tests

Figure 0.1. The Varina-Enon bridge (VEB).

3.1.2. Finite Element model

In this study, CSI Bridge was used to create a 3-D finite element model of three spans (5 to 7) of the VEB. These spans are significantly far from the cable-stayed portion, and therefore, the cable stays were ignored and only the external tendons were modeled. As explained in Subsection 3.1.1, in each span, there are eight tendons (four on the right side and four on the left side). Each tendon consists of nineteen 0.6-in-diameter strands. These were explicitly modeled with two equivalent tendons (one on the right side and one on the left side) with equivalent areas. Other important bridge components such as bridge bearings should also be modeled. Each span is supported by two square-shaped (91 by 91 cm) elastomeric bearings whose geometries are shown in Table 3.1. The bearings are modeled as elastic springs in vertical, horizontal, and rotational directions with stiffness values of 1143752, 1755, and 16270 KN/m, respectively.

Table 0.1. The bearing geometries.

Because there was no evidence about the concrete strength and core test was not possible, the value 50 Mpa (7500 psi) was chosen through iteration to match the results of experimental measurements, explained later further. A general overview of this model is shown in Figure 3.2. In this model, eight-node solid elements were employed for the box girders and piers. Also, the piers, with a cross-section of about 5.5 by 2.5 m and a height of 34 m, were fixed to the ground. A general maximum mesh size of 2.9 X 1.2 X 0.1 m, in longitudinal, transverse, and depth directions, respectively, was selected. However, as shown in Figure 3.2, the mesh size was significantly refined around the sensor positions, i.e., throughout the concrete box and in a width of 3.6 m around the sensor positions, to a maximum size of 0.2 X 0.4 X 0.1 m. Then, the mesh sizes were evaluated through a mesh sensitivity analysis to ensure that the results are not dependent on the selected mesh sizes.

As shown in Figure 3.1.c, two strain measurement points were selected, at the bottom of the top slab and on top of the bottom slab in 18.3 m from Pier 7 of the bridge (in span 6). To obtain the strain-time response under the traversing trucks, a time-history analysis was performed. Then, strain-time responses were simulated at desired points with a sampling rate of 33 Hz.

Additionally, the strain responses were extracted under two large truck crossing events. These events mirrored a set of experimental tests performed on the VEB in 2020. These are explained later in this chapter. To model the lanes (lanes 1,2, and 3), three centerlines (one for each lane) were defined with proper offsets from the longitudinal centerline of the bridge. Then, the lane width of 3.66 m was assigned to each lane's centerline. The model dimensions match the actual structures.

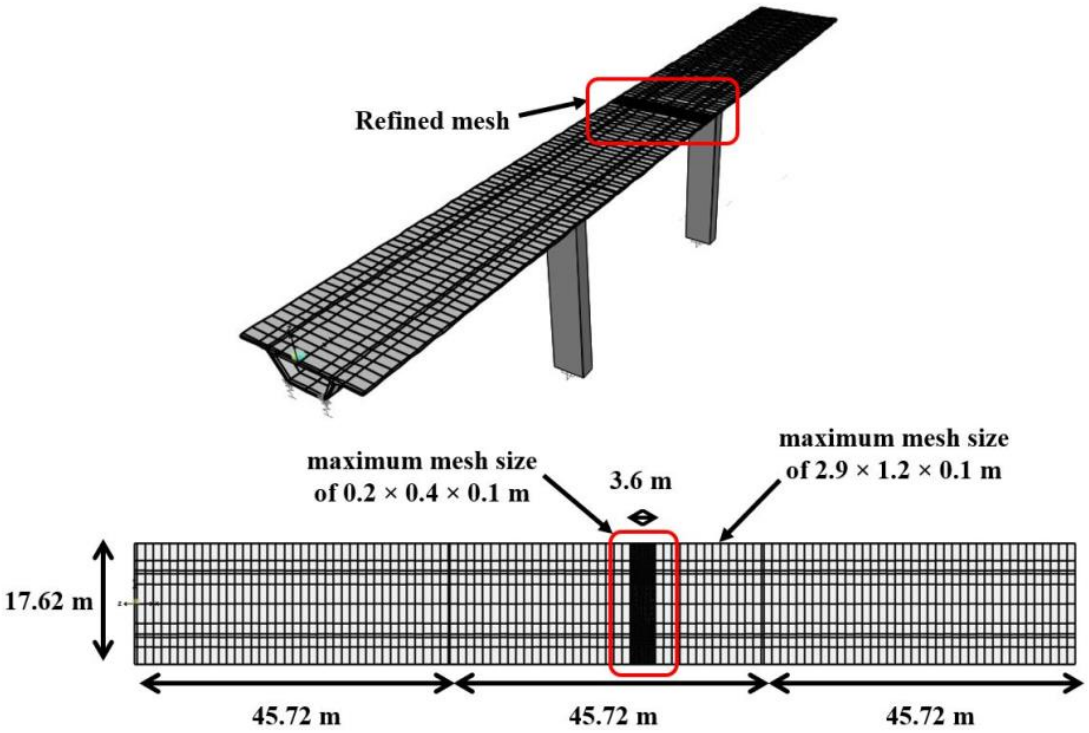

Figure 0.2. An overview of the finite element model.

3.1.3. Experimental Validation

To validate the FE model, experimental strain-time measurements, conducted on the VEB in 2020, were used. The responses (with a sampling rate of 33 Hz) were extracted at similar locations shown in Figure 3.1.c during large events' crossings. It should be noted that strain response is a very common response used for BWIM techniques. So, it was aimed to ensure that the strain response generated by the numerical model is fairly realistic and comparable with the strain response recorded on the actual bridge. That is why the strain response was the main factor for bridge model validation.

There were two large events in the experimental tests. The first event was a special permit vehicle, crossing over the second travel lane. All axle weights and axle spacings are shown in Figure 3.3.a. The second event was a superload test, with two lowboy trucks and two dump trucks, simultaneously crossing the VEB. Figures 3.3.b and 3.3.c show the general configurations for these truck types and more details are provided in Table 3.2. In this test, the two lowboys were on the third and second lanes and side-by-side to the two dump trucks traveled as close together as possible on the first lane.

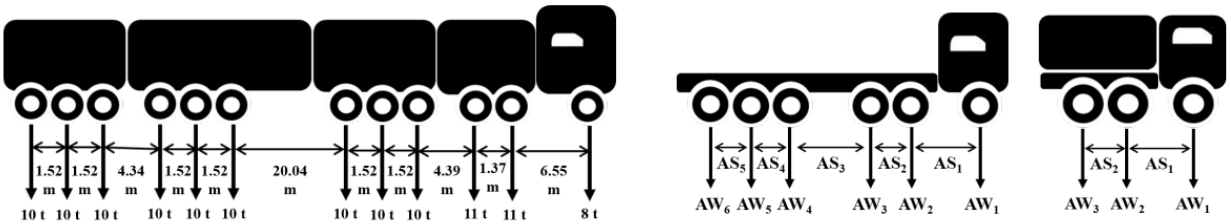

(c) Dump

(a) Special permit vehicle *(b) Lowboy truck* *truck*

Figure 0.3.Trucks used for FE model validation.

Table 0.2. Trucks' information for FE model validation in superload test (Figure 3.3).

Truck label	Truck name	No. of axles	Axle weight (ton)						Axle spacing (m)				
			AW_1[a]	AW_2	AW_3	AW_4	AW_5	AW_6	AS_1[b]	AS_2	AS_3	AS_4	AS_5
A	Lowboy 1	6	6.20	10.95	10.75	8.60	8.70	8.60	4.80	1.40	11.48	1.42	1.42
B	Lowboy 2	6	6.20	12.85	13.20	9.05	8.80	8.75	1.65	1.52	11.28	1.37	1.37
C	Dump 1	3	7.55	8.60	8.40	N/A	N/A	N/A	4.72	1.37	N/A	N/A	N/A
D	Dump 2	3	7.60	8.65	8.75	N/A	N/A	N/A	4.88	1.52	N/A	N/A	N/A

[a]AW=Axle weight, [b]AW=Axle spacing

The main purpose of this stage was to validate the FE model such that it provides similar general shapes for strain-time responses when it is under the same load, reasonable magnitudes (minimums and maximums), and captures the localized strains under the axles' weights. According to Figure 3.4, these requirements are satisfied, and experimental and numerical strain-time responses are in good agreement.

Also, in the experimental tests, there was no clear evidence about the trucks' speeds. Different speeds in the FE model than the tests stretch or compress the numerical strain responses if the trucks' speeds are assigned smaller or larger than the tests, respectively. To avoid this, in the FE model, the speeds were gradually changed until the time interval between the first and last peaks in Figure 3.4 became the same. Then, other peaks were automatically matched together.

According to Figure 3.4, despite a great match between experimental and numerical results, there are some discrepancies between them. These can be due to several reasons, including the slight difference in material properties (reported in design plans vs. actual material), different actual topping thickness than the design plans, and different bridge dimensions than the design plans. This can also be due to additional sources of error that are expected in an experimental setting, such as different trucks' transverse positions in the tests, different weights than the reported ones, different axles' configurations, etc. However, this model and the extracted strain-time responses were used for weight estimation. The discrepancies will not make any issue for it as long as the general shape and magnitudes are realistic. This is because both the IL calibration procedure (influence line extraction) and tests were done using the same model outputs.

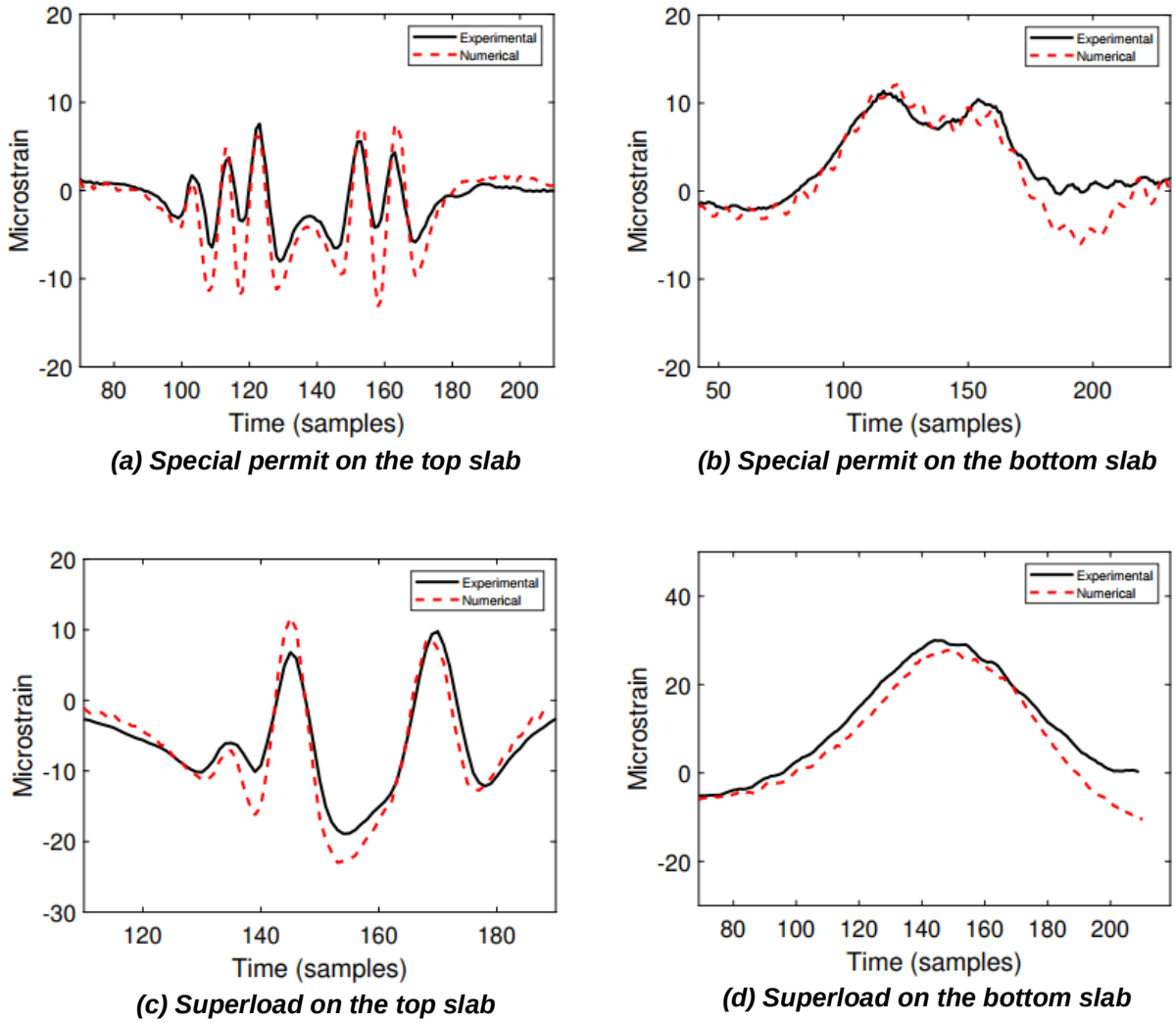

(a) Special permit on the top slab

(b) Special permit on the bottom slab

(c) Superload on the top slab

(d) Superload on the bottom slab

Figure 0.4. The FE model validation results.

3.2. Single and multiple-truck cases for MP NOR BWIM

In an actual situation, it is usually very challenging to control the traffic (without lane closure) to consider desired traffic load patterns with multiple trucks involved. Thus, in the rest of this study, the validated FE model was used to resolve this issue. In fact, this model enabled the consideration of complex traffic patterns and provided realistic strain-time responses. However, for the remainder of the report, sensor positions, sampling rate, and the vehicles used for weight estimation are different from the model validation section. These are described in the following subsections.

Also, before going through complex traffic patterns, as a proof-of-concept, it was first needed to show that the proposed approach works for single truck passages on lanes one or two. Subsection 3.2.1 is provided for this purpose.

3.2.1. Sensor position for weight estimation

To arrange a suitable sensor position for weight estimation, two assumptions were made. First, according to Virginia Code Title 46.2 (as defined in section 46.2-341.4), when the posted speed limit is at least 65 miles per hour (104.6 km/h), no commercial motor vehicle should be driven on the left-most lane of any interstate highway with more than two lanes in each direction [63]. This includes the Varina-Enon bridge as well. Thus, only the rightmost two lanes were considered for IL calibration and testing.

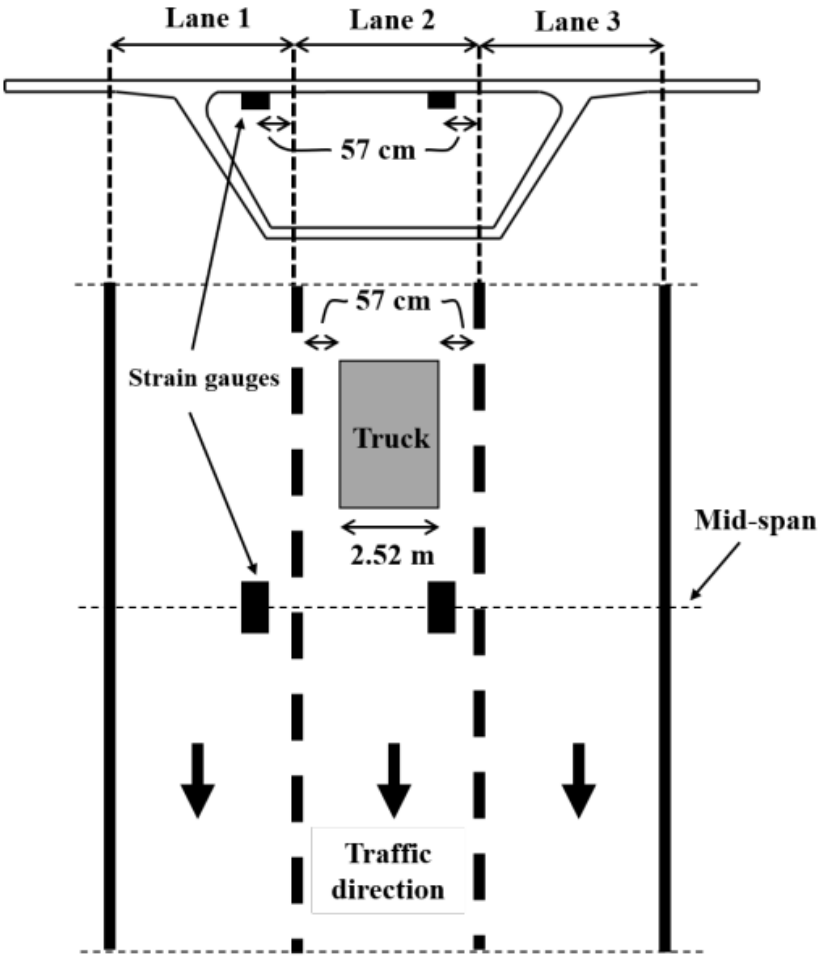

Figure 0.5. Sensor positions for weight estimation.

Second, according to a survey conducted by Berard and Bourion [64], the mean width of heavy trucks is 2.52 m, with approximately ninety percent of them within the range of 2.5 to 2.6 m. Also, according to the federal size regulations for commercial motor vehicles [65], the maximum width of commercial trucks is 2.6 m. Thus, as shown in Figure 3.5, for a standard lane width of 3.66 m (12 ft) and for a mean truck width of 2.52 m, the trucks' transverse position variability is going to be at most 57 cm if the strain gauges are placed in 57 cm from the pavement markings (at mid-span). This sensor placement enables one to capture most of the localized portion of the strains under the trucks' tires. Thus, the strain response is expected to consist of clear peaks, and a slight change in trucks' transverse positions (within a range of ±57 cm) should not damage the peaks' clarity. The results are shown later in the next sections.

Also, for the rest of this paper, i.e., weight estimation for single and multiple-truck cases, the sampling rate is 100 Hz. This is different from the sampling rate for model validation (33 Hz).

3.2.2. Single-truck cases

As mentioned earlier, it was first needed to compare the weight estimation results from the proposed BWIM approach with standard BWIM methods (as a proof-of-concept) for single-truck cases. For both the standard and proposed approaches, two separate influence lines, i.e., IL1 and IL2, were extracted for lanes one and two. This was done using Truck 1 in Table 3.3 (different than the validation trucks) with multiple passages in different transverse positions.

Once the influence lines were obtained, Trucks 2 through 6, introduced in Table 3.3, were passed one by one on the first and second lanes, and ten strain-time responses (five for each lane) were obtained. In the last step, two different approaches (the standard BWIM and proposed BWIM), already discussed in previous sections were applied, and axle weights and GVWs were computed. Then, the results were compared together shown later in the next sections.

Table 0.3. Trucks' information for weight estimation (single and multiple-truck cases).

Truck no.	No. of axles	Axle weight (ton)					GVW (ton)	Axle spacing (m)			
		AW_1[a]	AW_2	AW_3	AW_4	AW_5		AS_1[b]	AS_2	AS_3	AS_4
1	3	8.2	7.5	7.5	N/A	N/A	23.2	4.60	1.25	N/A	N/A
2	3	9.1	7.1	7.1	N/A	N/A	23.3	4.50	1.31	N/A	N/A
3	5	4.5	7.1	7.1	7.1	7.1	32.9	3.35	1.22	6.71	1.22
4	5	6.2	8.0	8.2	8.0	8.2	38.6	3.40	1.31	6.78	1.31
5	4	5.1	8.3	8.3	10.4	N/A	32.1	3.60	1.20	6.60	N/A
6	4	5.3	7.0	7.0	8.5	N/A	27.8	3.70	1.32	7.00	N/A

[a]AW=Axle weight, [b]AW=Axle spacing

3.2.3. Multiple-truck traffic patterns

Once it is proved that the proposed BWIM approach works for single-truck cases, more complex traffic patterns should also be tested. As shown in Figure 3.6, six different traffic patterns with multiple simultaneous vehicles' presence (trucks and light-weight vehicles) were considered for multiple-truck cases. These traffic patterns were including two in-one-row cases (Figures 3.6.a and 3.6.b) with a 5-axle and a 3-axle trucks, two zigzag cases with three 3-axle trucks (Figures 3.6.c and 3.6.d), a zigzag case with two 3-axle trucks and a 5-axle truck on the first two lanes and two light-weight vehicles on the third lane (Figure 3.6.e), and a side-by-side case with a 5-axle and a 3-axle trucks on the first and second lanes, respectively. In all cases, the 3-axle and 5-axle trucks were Trucks 2 and 4, respectively, described in Table 3.3. Also, the light-weight vehicles were both a 2-axle vehicle with axle spacing of about 4 m and equal axle weights of 0.6 ton (GVW=1.2 ton).

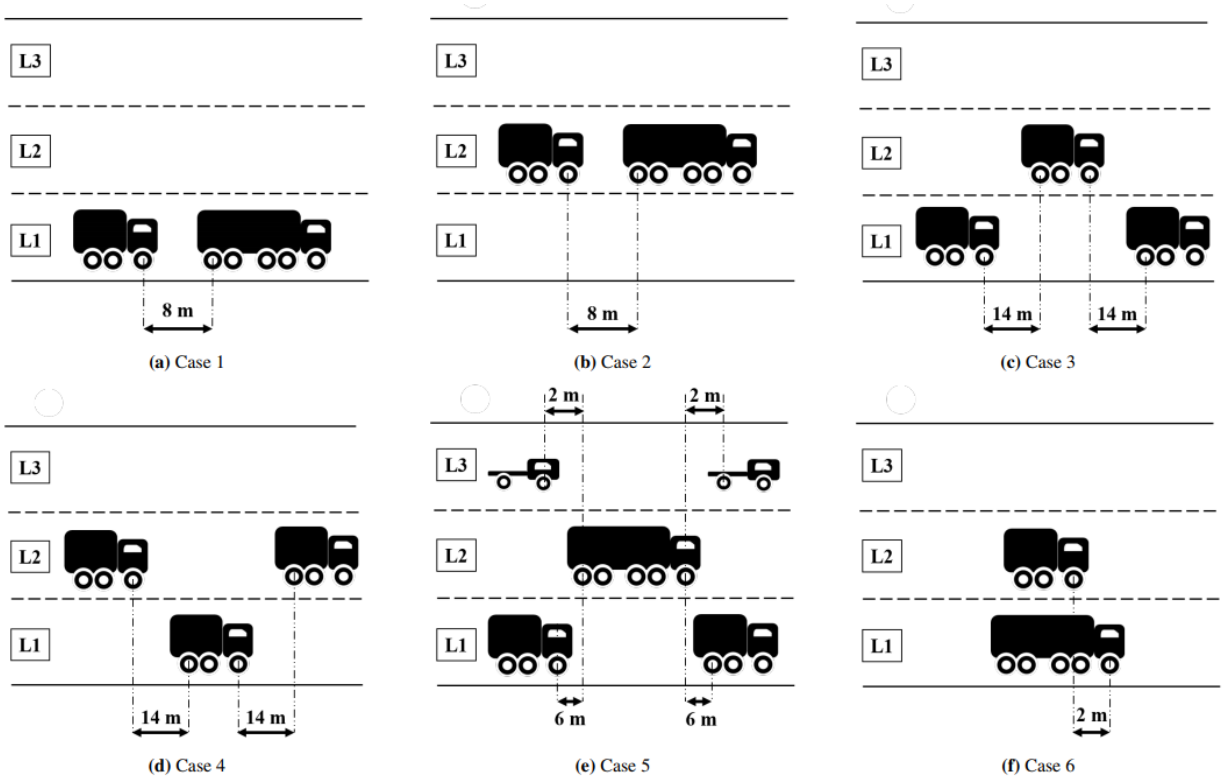

Table 0.4. Multiple-truck cases (the 3-axle and 5-axle trucks are Trucks 2 and 4 described in Table 3.3).

3.3. The analysis approach for the dual-purpose SHM procedure

A similar 3-D finite element (FE) model was used with some modifications. This phase was conducted after the MP NOR BWIM technique evaluation phase. Only two spans (spans 5 and 6) of the VE bridge were modeled. In the previous model, three spans (spans 5 to 7) were simulated as a continuous superstructure, while there is an expansion joint between spans 6 and 7 on the real VE bridge. Thus, the latter one was removed in this phase to create a more realistic model.

The measurement points for SHM were selected at mid-span (span 6) and in a transverse position of 57cm from the pavement markings. The sampling rate was also 100 Hz, similar to the MP NOR BWIM evaluation.

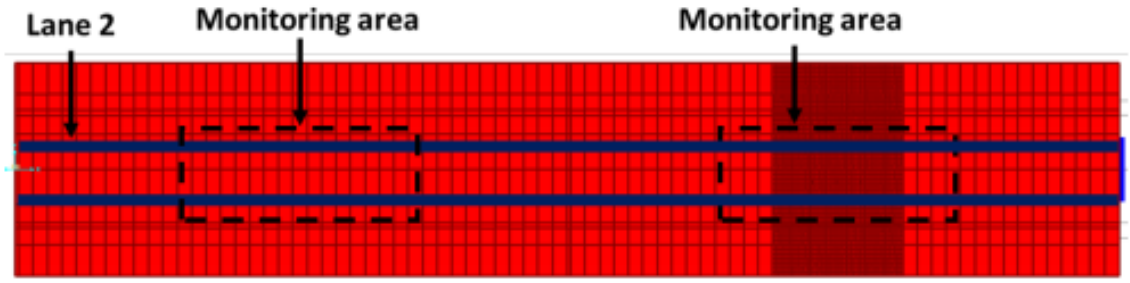

(a) The Monitoring area

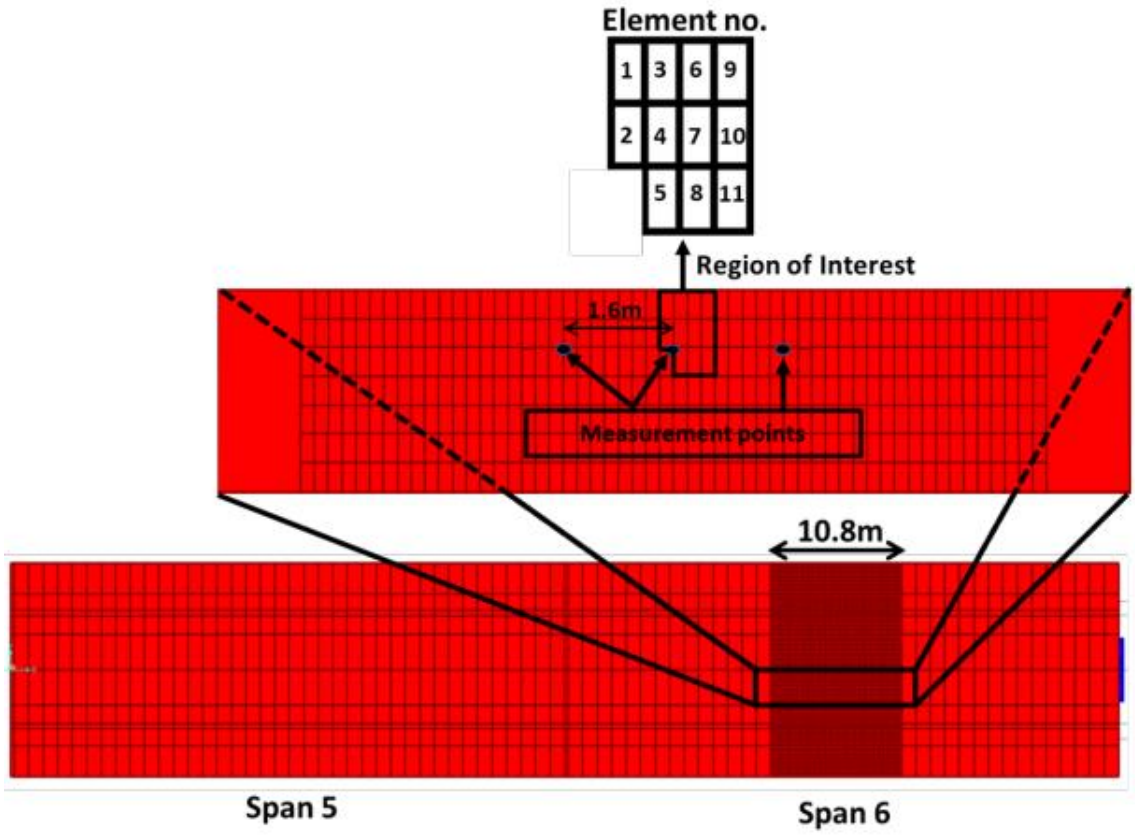

(b) The region of interest

Table 0.5. Region of interest and measurement points.

This study evaluates the MP-IL to see if it can effectively address the multiple-presence issue of the standard BWIM techniques and adequately obtain the trucks' axle weights even in highly complicated traffic conditions. This study shows the capability of the same BWIM system but also to be used for bridge health monitoring. A common practice for BWIM systems is to use at least three sensors (such as strain gauges) to obtain the prerequisites (i.e., speed, number of axles, and axle spacing) to be later used for weight estimation. As shown in Figure 3.7, the distance between the successive strain gauges is suggested to be 1.6 m in this study, which is in good agreement with the papers published in the BWIM area [22], [24].

The goal is to monitor the integrity of the concrete-box top slab and the area where maximum local (under tires) and global deflections (maximum tension in concrete) usually happen (shown in Figure 3.7.a). Due to symmetry, only the top right quadrant of the second measurement point is evaluated, and the results will be extended to other quadrants around the measurement point. This is called ``Region of Interest (ROI)" shown in Figure 3.7.b. This study results from more than 90 truck passages in CSI Bridge software with more than 110 hours of effective analysis time (more than 70 minutes each). Considering the ROI and extending the results reduced the analysis time significantly.

To model different damage scenarios, eleven different elements (in the ROI) shown in Figure 3.7.b were removed one by one, and separate analyses were performed (each analysis with only one removed element). These are called damage scenarios 1 through 11. This was to understand how sensitive the monitoring system and the proposed dual-purpose approach are to different damage locations. Later, depending on the monitoring system's effectiveness in the damage locations, the sensor placement and their distances are updated to more effectively monitor the top slab and to be still suitable for the BWIM application. This is discussed later in the next section. It should be noted that top slab monitoring is only an example to show the capability of the integrated system and can be extended to other damage scenarios as well. This is left for future studies.

The key computation for bridge health monitoring using the dual-purpose procedure is the change occurred in the ILs of the bridges at the monitoring stage compared to the reference ILs (IL1 and IL2). To obtain the reference ILs, several SHM trucks with different axle configurations and weights should move through the intact bridge to obtain the strain-time responses. The sampling rate was selected to be 100 Hz, suggested by other studies [62]. In this study, three trucks (a 3-axle, a 4-axle, and a 5-axle), shown in Figure 3.8 were selected.

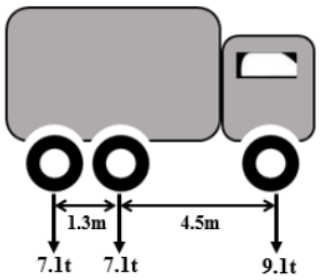

(a) The 3-axle truck

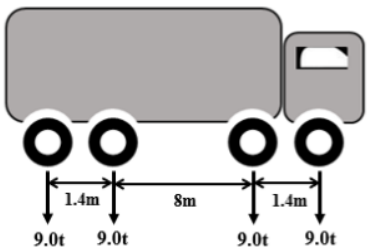

(b) The 4-axle truck

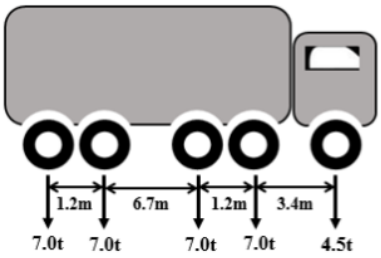

(c) The 5-axle truck

Table 0.6. SHM trucks

As a proof of concept, the strain response of the intact bridge and its corresponding IL under the 3-axle truck are plotted against the strain response and IL under the same 3-axle truck but with doubled axle weights. This is shown in Figure 3.9. According to this figure, the strain responses (both localized and non-localized) are significantly different; however, the IL still remained unique for this bridge. This shows why IL is selected for SHM and not strain response.

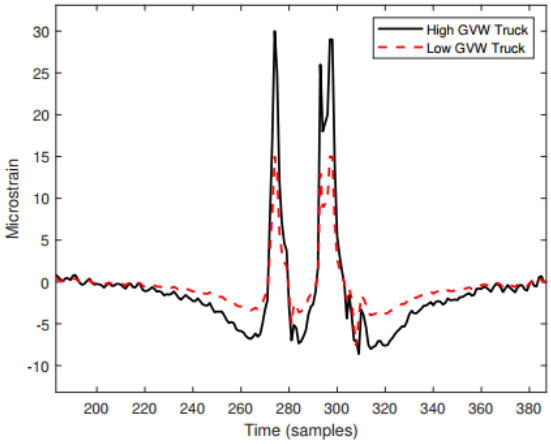

(a) Strain responses

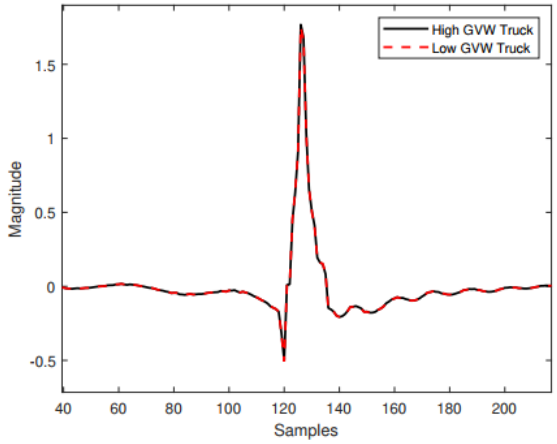

(b) Influence lines

Table 0.7. Comparison of the strain responses and ILs for the same trucks but with significantly different GVWs.

It was also discussed already that factors such as noise and the transverse position may change the IL of the bridge and can create fake non-zero DIs even for the intact bridge. Thus, these factors were included in the analysis explained below.

The first step in considering the transverse position was to compute a reasonable range for its variability. According to a survey [64], the mean width of heavy trucks is 2.52 m, with approximately 90% from 2.5 to 2.6 m. Also, the maximum width of commercial trucks is 2.6 m [65]. Thus, the trucks' transverse position variability is a maximum of 57 cm for a standard lane width of 3.66 m (12 ft). Also, the bridge monitoring is usually an under-control evaluation process, and the SHM truck drivers can be requested to possibly drive on the center of the lanes. Thus, it is reasonable to consider a smaller value than 57cm for the transverse position change. In this study, a maximum of ±30 cm was considered only to include the drivers' accuracy in the procedure.

A significant amount of noise was then added to the strain-time responses from all variations of the trucks' transverse positions (three for each truck and a total of nine responses). In this study, the “randn"” function in MATLAB was used to generate signals with normally distributed random numbers that were then added to the original strain responses.

Once the strain-time responses were obtained, standard IL and MP-IL approaches were applied to the noisy responses (for each truck) on different transverse positions to obtain the ILs. Thus, for each truck, two reference ILs were extracted, one using the standard BWIM method (for single-truck events) and the other using MP-IL (for multiple-truck events). ILs 1 and 2 were later used for future monitoring.

Once the reference ILs were extracted, two DI thresholds, one for single-truck events and the other for multiple-truck events (called thresholds 1 and 2, respectively), were computed for each truck type. A 95% confidence analysis was performed on the DIs calculated using the ILs extracted from the intact bridge on different transverse positions and subjected to different noise levels. Both thresholds 1 and 2 were from the intact bridge but under single-truck events and multiple-truck events (SHM truck

surrounded by unwanted trucks), respectively. If the DI values (at the monitoring stage) come up to be greater than the thresholds, it can be concluded that damage has occurred with 95% confidence; otherwise, we will not have enough evidence to conclude that damage has necessarily occurred even for non-zero DI values.

In the second step of the dual-purpose procedure, discussed in methodology section, the same trucks introduced in Figure 3.8 were again used on the damaged bridge. For each damage scenario and truck, a separate analysis was performed and the strain response was obtained (33 responses overall). Similar to the first step (Calibration on the Intact Bridge), for single-truck events and multiple-truck events, standard IL and MP-IL were used and the ILs of the damaged cases were obtained. The DIs were then computed and compared with the DI thresholds. The goal was to understand if the proposed dual-purpose procedure is sensitive to different damage scenarios under single and multiple events. Also, it was aimed to understand in what distance from the measurement point, the procedure can still provide reliable results for this particular damage intensity. Based on the results, the instrumentation plan is later updated to be effective for both the BWIM and SHM applications.

Table 0.8. Different configurations of the 3axle truck used for parametric study.

Case no.	Truck no.	Axle weight (ton)			GVW (ton)	Axle spacing (m)	
		AW_1[a]	AW_2	AW_3		AS_1[b]	AS_2
1	1	18.20	14.20	14.20	46.6	4.5	1.3
	2	13.65	10.65	10.65	34.95	4.5	1.3
	3	6.07	4.73	4.73	15.53	4.5	1.3
	4	4.55	3.55	3.55	11.65	4.5	1.3
2	5	9.10	7.10	7.10	23.30	6.0	1.3
	6	9.10	7.10	7.10	23.30	3.0	1.3
3	7	11.10	6.10	6.10	23.30	4.5	1.3
	8	13.10	5.10	5.10	23.30	4.5	1.3
	9	7.10	8.10	8.10	23.30	4.5	1.3
	10	7.77	7.77	7.77	23.30	4.5	1.3
	11	16.10	3.60	3.60	23.30	4.5	1.3

[a]AW=Axle weight, [b]AS=Axle spacing

As mentioned earlier, the proposed dual-purpose procedure should be repeated with different trucks with different configurations and weights. It is later shown in results section that this can improve the bridge integrity monitoring results. To understand the reason why this improvement happens, a parametric study was performed to consider the effect of different factors on DI values. When the type of truck is changed (from a 3-axle to a 5-axle, for instance), three factors may change: 1) gross vehicle weight, 2) axle weights 3) axle spacings. Thus, the 3-axle truck shown in Figure 3.8.a was used as a reference, and its characteristics were changed one by one, and the DI values were compared with the reference 3-axle truck. Table 3.4 shows three different cases to consider the effect of the trucks' characteristics on the DI value. In Case 1, the gross vehicle weights (GVW) were changed compared to the reference 3-axle truck, but the axle weight ratios and axle spacings were the same. In Case 2, the GVWs and axle weight ratios were the same, and only the first axle spacings were altered, while in Case 3, only the axle weight ratios were changed, and the other two factors remained constant.

CHAPTER 4

Phase I findings

INTRODUCTION

This section reports the results of MP NOR-BWIM technique to understand if it can handle multiple-truck events and complex traffic patterns.

4.1. Single-truck cases

Before considering the multiple-truck cases, it was first needed to compare the performance of the proposed approach with the standard BWIM method in single-truck cases. This is to ensure that the non-localized strain removal does not sacrifice the accuracy of results much (the accuracy reduction is in a reasonable range). Hence, ten strain-time responses were obtained for Trucks 2 through 6, introduced in Table 3.3 (for each truck two responses, one in lane one and another one in lane two). As mentioned earlier, Truck 1 was used for influence line extraction. Then, the standard BWIM and proposed BWIM, discussed in Chapter 2, were applied to the responses.

The estimated axle weights, estimated GVW, and their associated errors are shown in Table 4.1 for both approaches and lanes. According to this table, overall, the proposed approach improved the GVW estimation compared to the standard approach. The mean absolute errors (MAE) of the axle weights and GVW estimates for the standard approach were 4.1% and 4.8%, respectively, when the truck was on lane one. These errors were 2.2% and 7.4% for the same lane but the proposed approach. Additionally, MAEs of the axle weights and GVW estimates for lane two and the standard approach were 4.8% and 6.5% versus 2.4% and 10.6% for the same lane but the proposed approach. Hence, as mentioned above, the proposed approach improved the GVW estimation accuracy by 1.9% and 2.4%, respectively, for lanes one and two; however, it reduced the axle weight estimation accuracy by 2.6% and 4.1%. This increase in axle weight estimation error can be ignored since the GVW estimation accuracy is improved and multiple-truck weight estimation is enabled. Also, axle weight errors are still in a reasonable range. Thus, one can conclude that removing the non-localized strain does not eliminate much important information.

Overall, for both standard and proposed approaches, the average absolute errors of GVW and axle weight estimates were greater for lane two than lane one. However, the errors' magnitudes are not consistently greater for all trucks in lane two than lane one. In this study, two main factors were detected for variability in errors.

1) Similarity of the characteristics of the test and calibration trucks: it was observed that the error is close to zero when the same truck is used for both IL calibration and test. However, when the test truck characteristics (e.g., axle spacings, number of axles, etc.) are different from the calibration truck, both standard and proposed techniques are still capable of generating a strain response with great match with respect to the original one, but with more dispersion (compared to the case with the same test and calibration trucks). When the reconstructed strain is consistently above/under the original strain, a larger positive/negative error will result for both GVW and axle weight estimates. However, when at some points, it is above and at other points it is under the original response, the positive and negative GVW

errors cancel out each other, and a small GVW error (close to zero) will result, but still, large axle weight errors are likely (depending on the level of dispersion). 2) The effect of smoothing technique for different strain responses: in this study, it was confirmed that the errors would be overall smaller when the strain responses are smoothed using ``Symlets Wavelet'' (sym4 with a level of wavelet decomposition of 2 in MATLAB). However, as mentioned earlier, its effect can still be variable for different responses.

In short, the errors due to these two factors can be cumulative (for the same error sign) or balancing (for opposite error signs). This is why different errors with different signs and values are observed from case to case and lane to lane.

Table 0.1. The results of single-truck cases.

App.[a]	L.[b] no.	Ax.[c] no.	Truck 1		Truck 2		Truck 3		Truck 4		Truck 5		Ave. err.*	
			Est.[d] (ton)	err.[e] (%)	Est. (ton)	err. (%)	Est. (ton)	err. (%)	Est. (ton)	err. (%)	Est. (ton)	err. (%)	GVW[f] (%)	Ax. (%)
Std.[g]	1	1	8.98	-1.3	4.32	-4.0	6.01	-3.1	4.14	-18.8	4.89	-7.8	4.1	4.8
		2	7.16	0.9	6.79	-4.3	8.08	1.0	8.56	3.1	6.77	-3.2		
		3	6.63	-6.6	6.85	-3.6	8.02	-2.3	6.67	-19.6	6.53	-6.7		
		4	N/A	N/A	7.11	0.1	7.84	-2.0	9.52	-8.5	8.44	-0.7		
		5	N/A	N/A	6.90	-2.8	8.14	-0.7	N/A	N/A	N/A	N/A		
		GVW	22.77	-2.3	31.96	-2.8	38.09	-1.3	28.89	-10.0	26.63	-4.2		
Std.	2	1	8.82	-3.1	4.21	-6.5	5.90	-4.9	4.30	-15.7	4.74	-10.7	4.8	6.5
		2	7.41	4.4	6.69	-5.8	8.16	2.0	8.85	6.6	7.14	2.1		
		3	6.61	-6.9	6.80	-4.2	7.69	-6.2	6.20	-25.3	6.09	-13.0		
		4	N/A	N/A	7.13	0.4	7.73	-3.3	9.56	-8.1	8.09	-4.8		
		5	N/A	N/A	6.93	-2.4	8.24	0.5	N/A	N/A	N/A	N/A		
		GVW	22.84	-2.0	31.76	-3.5	37.72	-2.3	28.90	-10.0	26.06	-6.2		
Prop.[h]	1	1	9.45	3.9	4.36	-3.1	5.39	-13.1	5.04	-1.3	5.41	2.0	2.2	7.4
		2	7.15	0.7	6.16	-13.2	8.26	3.3	7.72	-6.9	6.54	-6.6		
		3	6.50	-8.4	7.80	9.8	6.38	-22.2	8.20	-1.1	7.19	2.7		
		4	N/A	N/A	6.25	-12.0	8.61	7.6	10.88	4.6	8.49	-0.2		
		5	N/A	N/A	8.15	14.8	6.80	-17.0	N/A	N/A	N/A	N/A		
		GVW	23.10	-0.8	32.72	-0.5	35.44	-8.2	31.9	-0.8	27.62	-0.7		
Prop.	2	1	9.26	1.8	4.14	-8.0	6.39	3.0	4.93	-3.3	5.84	10.1	2.4	10.6
		2	7.90	11.3	6.13	-13.7	10.29	28.7	7.96	-4.1	6.92	-1.2		
		3	6.378	-10.3	8.03	13.1	6.24	-23.9	8.17	-1.6	7.57	8.1		
		4	N/A	N/A	6.29	-11.5	9.85	23.1	10.54	1.3	8.52	0.3		
		5	N/A	N/A	9.18	29.3	6.92	-15.6	N/A	N/A	N/A	N/A		
		GVW	23.54	1.0	33.76	2.6	39.69	2.8	31.59	-1.6	28.85	3.8		

[a] Approach,[b] Lane,[c] Axle,[d] Estimate,[e] error,[f] gross-vehicle-weight,[g] Standard,[h] Proposed

* Note: Average absolute error calculated based on all five cases for each lane and approach

4.2. Multiple-truck cases

This section shows that the proposed approach also works accurately for multiple-truck cases. According to Subsection 3.2, six different cases were considered (shown in Figure 3.6). Overall, considering all trucks in all six cases, the mean absolute errors were 4.50% and 11.3% for GVW and axle weight estimations. The details are provided in Table 4.2.

Table 0.2. The results of multiple-truck cases.

Case no.	Axle no.	Truck 1		Truck 2		Truck 3	
		Est. (ton)	error (%)	Est. (ton)	error (%)	Est. (ton)	error (%)
1	1	9.21	1.2	5.80	-6.5	N/A	N/A
	2	7.38	3.9	7.99	-0.15	N/A	N/A
	3	5.23	-26.3	7.35	-10.4	N/A	N/A
	4	N/A	N/A	8.57	7.1	N/A	N/A
	5	N/A	N/A	8.49	3.6	N/A	N/A
GVW		21.82	-6.4	38.19	-1.1	N/A	N/A
2	1	8.79	-3.4	6.09	-1.8	N/A	N/A
	2	8.56	20.5	8.88	11.0	N/A	N/A
	3	4.89	-31.2	7.11	-13.3	N/A	N/A
	4	N/A	N/A	8.57	7.2	N/A	N/A
	5	N/A	N/A	8.53	4.0	N/A	N/A
GVW		22.24	-4.6	39.17	1.5	N/A	N/A
3	1	10.00	9.9	9.61	5.7	9.96	9.4
	2	8.02	12.9	8.07	13.7	7.74	9.0
	3	6.89	-2.9	6.15	-13.4	6.62	-6.8
GVW		24.91	6.9	23.83	2.3	24.32	4.4
4	1	9.52	4.7	10.18	11.9	10.19	11.9
	2	8.11	14.2	7.29	2.7	8.56	20.5
	3	6.35	-10.6	7.20	1.3	6.41	-9.7
GVW		23.98	2.9	24.67	5.9	25.16	8.0
5	1	9.19	1.0	9.65	6.1	6.57	5.9
	2	8.22	15.8	8.38	18.1	10.61	32.6
	3	5.94	-16.4	5.95	-16.2	6.38	-22.2
	4	N/A	N/A	N/A	N/A	10.60	32.5
	5	N/A	N/A	N/A	N/A	7.37	-10.2
GVW		23.35	0.2	23.99	3.0	41.51	7.6
6	1	9.68	6.3	6.77	9.3	N/A	N/A
	2	7.12	0.3	9.90	23.8	N/A	N/A
	3	4.03	-43.2	8.09	-1.3	N/A	N/A
	4	N/A	N/A	7.63	-4.6	N/A	N/A
	5	N/A	N/A	7.13	-13.0	N/A	N/A
GVW		20.83	-10.6	39.53	2.4	N/A	N/A

Note: The overall mean absolute errors, based on all six multiple-truck cases, for axle weight and GVW estimations, were 11.36% and 4.43%, respectively.

Figure 4.1 shows the results for Case 1, where two trucks, i.e., a 5-axle and a 3-axle, with a longitudinal distance of 8 m, simultaneously passed through the first lane. Figure 4.1.a shows the original strain response and the fitted curve to its non-localized portion. According to this figure, when the sensors are placed where maximum localized strain occurs, the axles can be successfully captured even for closely-spaced ones. Additionally, Figure 4.1.b shows the modified strain response (when the non-localized portion of the strain is removed) and the selected portions needed for weight estimation. The same procedure was conducted for Case 2, where the same trucks with the same distance passed through the second lane. The results are shown for both cases in Table 4.2. According to this table, the GVW estimation errors for Case 1 were -6.4% and -1.1% for the 3-axle and 5-axle trucks, respectively, while they were -4.6% and 1.5% for Case 2. Thus, overall, except for the 5-axle truck in Case 2, GVWs were all underestimated. Also, in both cases, the GVW estimation errors associated with the 3-axle trucks were greater than the 5-axles. Additionally, considering all axles of both 3-axle and 5-axle trucks, lane two

generated greater axle weight errors than lane one (11.6% vs. 7.4%); however, in average, GVW error associated with lane one (3.8%) was greater than lane two (3.1%). Similar to the GVW errors, the axle weights errors are also greater for the 3-axle compared to the 5-axle trucks in both cases. The reason for the variability of errors was already discussed in Subsection 4.1.

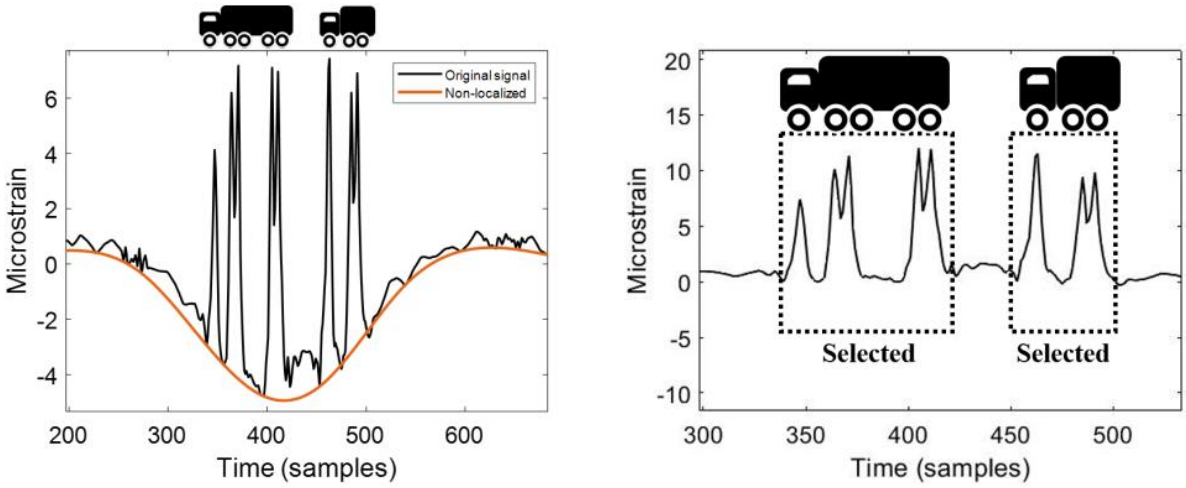

(a) The original strain-time response

(b) The proposed approach result (selected portions)

Figure 0.1. Case 1: a 5-axle truck and a 3-axle truck on the lane one

For Case 3, which is a zigzag pattern with two 3-axle trucks on the first lane and a 3-axle truck on the second lane, only the modified strain response (non-localized portion removed) and the selected portion for weight estimation are shown (for conciseness). Figures 4.2.a and 4.2.b respectively show the modified strain responses and the selected portions for weight estimation on lanes one and two. Also, as explained earlier, when two trucks move on two adjacent lanes, the strain response will be a combination of sharp peaks due to the trucks on the same lane and distorted peaks due to the reflection of the truck on the adjacent lane. This is clearly shown in Figure 4.2. Only the portions with sharp peaks were used for weight estimation and the distorted parts were discarded. This was already explained in detail in Chapter 2. The same procedure was performed for Case 4 with a zigzag pattern with one 3-axle truck on the first lane and two 3-axle trucks on the second lane. Table 4.2 shows the results for both cases. According to this table, the GVW estimation errors for Case 3 were 6.9% (lane one), 2.3% (lane two), and 4.4% (lane one) for the left, middle, and right 3-axle trucks while they were 2.9% (lane two), 5.9% (lane one), and 8.0% (lane two) for Case 4. Thus, in average, lane two generated smaller GVW errors compared to lane one. Also, the mean absolute errors for axle weight estimation were similar values of 9.3% and 9.7% for Cases 3 and 4, respectively (considering all axles and all trucks for each case). However, in average, lane 2 generated greater axle weight errors (11.6%) compared to lane one (7.4%), considering both Cases 3 and 4 together.

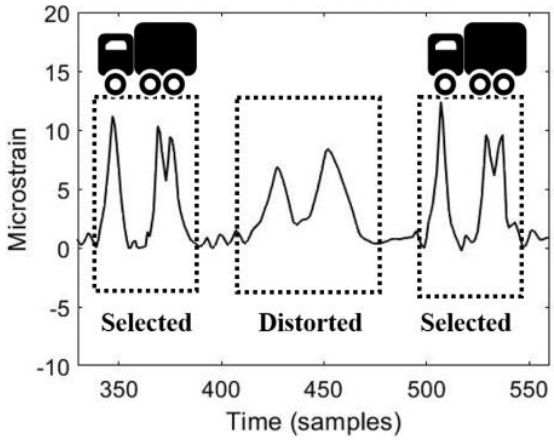

(a) The selected and discarded portions in the response from Lane 1

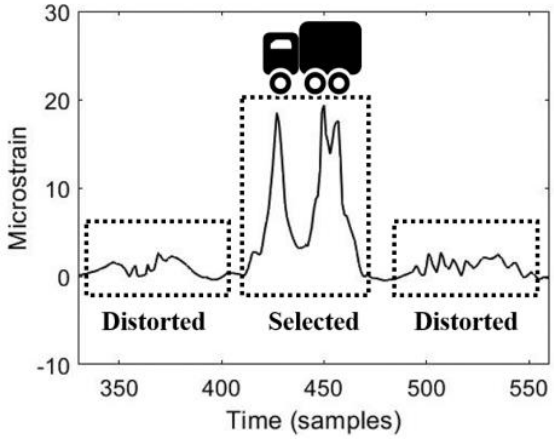

(b) The selected and discarded portions in the response from Lane 2

Figure 0.2. Case 3: a zigzag pattern with two 3-axle trucks on the first lane and a 3-axle truck on the second lane.

Case 5 is a zigzag pattern with two 3-axle trucks on the first lane, a 5-axle truck on the second lane, and two light-weight vehicles on the third lane. Similar to Cases 3 and 4, the strain responses from lanes one and two were decomposed, and the distorted portions (adjacent truck reflection) were excluded and only the portions with sharp peaks were selected. The light-weight vehicles (total weight of 1.2 tons), due to their small weights, did not have a considerable reflection on the responses extracted from lanes one and two. According to Table 4.2, the GVW estimation errors were 0.2% (lane one), 3% (lane one), and 7.6% (lane two) for the two 3-axle trucks and the 5-axle truck, respectively. Thus, overall, the 5-axle truck and lane two generated greater GVW errors. The axle weight error for the 5-axle truck on the second lane (20.68%) was overall greater than the 3-axle trucks on the first lane (12.3%).

Case 6 is a 5-axle truck and a 3-axle truck in two adjacent lanes moving side-by-side at a longitudinal distance of 2 m. As explained in Chapter 2, for side-by-side trucks, the strain response has a combination of clear and distorted peaks, and only the clear peaks should be kept and the remaining should be removed. This was already explained in detail in Chapter 2. According to Table 4.2, the GVW estimation errors were -10.6% (lane two) and 2.4% (lane one) for the 3-axle and the 5-axle trucks, respectively. Additionally, the mean absolute error for axle weight estimation was 12.7%.

In general, different factors can contribute to the weight estimation error: 1) truck type (3-axle vs. 5-axle), 2) truck weight, 3) different lanes 4) transverse position and 5) temperature change. In this study, the first three factors were simultaneously changing, making the parametric study difficult. Here, a preliminary parametric study is conducted for the first three factors and further discussion is left for a future study where these factors change one by one.

Overall, in all these six cases, the 3-axle truck (lighter) eleven times and the 5-axle truck (heavier) four times were used. According to the results, in both GVW and axle weight estimations (considering all six cases), the proposed approach was, on average, more successful on the 5-axle truck compared to the 3-axle truck. The average GVW and axle weight errors were respectively 5.0% and 11.5% for the 3-axle truck and 3.2% and 11.0% for the 5-axle truck. Also, in 4 cases (Cases 1,2,5, and 6), the 3-axle truck was directly compared with the 5-axle truck. In three out of four cases (Cases 1,2, and 6), GVW estimation was more accurate for the 5-axle truck, and in only one case (Case 5), it was more accurate for the 3-axle

truck. This was the same for axle weight estimation. A similar comparison can be used to discuss the effect of truck weight (factor 2 mentioned above) since the 5-axle truck is heavier than the 3-axle truck.

In this study, lanes one and two were both tested. It was observed that (for both GVW and axle weight estimations), the proposed approach was, on average, more accurate on lane one compared to lane two. The average errors for GVW and axle weight were 4.3% and 9.3% for lane one and 5.7% and 14.0% for lane two. Also, two other important factors are temperature change and the transverse position of the trucks (factors 4 and 5).

As explained earlier, the proposed BWIM method focuses on the localized strain portion. Also, the localized portion, particularly the peaks' values, can be affected by the truck transverse position and temperature change. These are out of the scope of this study but should be considered in a future study.

The main limitation for the proposed BWIM approach is going to be for a case where two side-by-side trucks with exactly the same axle configurations (axle spacing and the number of axles) crossing over the sensors at exactly the same time. In this case, the strain responses' peaks will align with each other and will not be straightforward to decompose. However, this can rarely happen as the accuracy of the data acquisition timestamp is 0.001 s. Thus, even if both trucks are exactly the same, there will most likely be some time delay between the truck positions and their peaks in the strain responses in the real situation. Overall, as mentioned earlier, the mean absolute errors, considering all trucks in all six cases, were respectively 4.5% and 11.3% for GVW and axle weight estimations. This shows that the proposed approach is capable of computing the axle and gross vehicle weights accurately, even for complex traffic load patterns with a combination of trucks and lightweight vehicles.

CHAPTER 5

Phase II findings

INTRODUCTION

This section reports the results of dual-purpose SHM procedure on single and multiple-truck events.

5.1. Reference ILs and thresholds

As discussed earlier in Chapter 3, the first step is to compute two reference ILs (IL1 and IL2) for each truck type to include the effect of noise and transverse position. Then, any change in a future IL (denoted as DI) from the bridge can be a sign of damage as long as it is greater than the DI thresholds.

To obtain the reference ILs, the SHM trucks (shown in Figure 3.8) moved through the intact bridge in different transverse positions (introduced earlier) and with different noise contents. Then, the standard IL and MP-IL techniques were applied to obtain a single reference IL for each truck, considering all transverse positions. Figures 5.1.a and 5.1.b compare the reference IL1 and 2, respectively, against the ILs extracted from a single 5-axle and two 5-axle trucks on the intact bridge. The shape of the reference ILs are obviously different since IL1 is obtained using the entire strain response while IL2 is obtained only using the localized portions.

In the next step, 54 different analyses were performed for the single and multiple-truck cases (27 for each) on the intact bridge and different transverse positions and with different noise contents. Then, the DIs and, accordingly, the DI thresholds were computed for each event type and truck. All these are shown in Table 5.1. As an example, the confidence interval (95% confidence) for the single 5-axle truck is 0.039 ± 0.008, with an upper limit (threshold) of 0.047. A future DI value greater than the thresholds can be a sign of damage with 95% confidence, and any value less than them cannot be certain evidence for damage and can be a fake non-zero DI value.

According to Table 5.1, overall, the noise and transverse position factors can make a maximum DI variation of 0.068 and 0.4 for the single-truck and multiple-truck events, respectively.

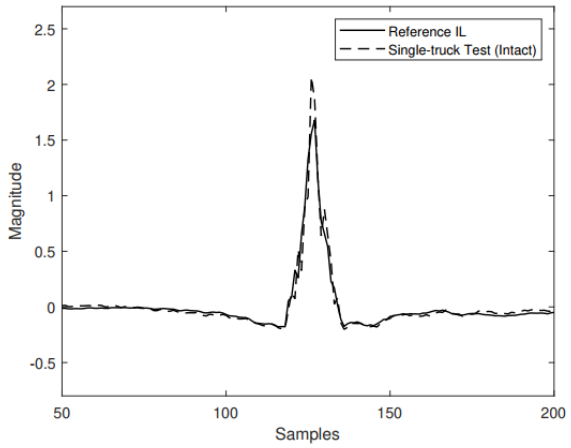

(a) Reference IL1 vs. the IL of a single-truck event (a 5-axle truck).

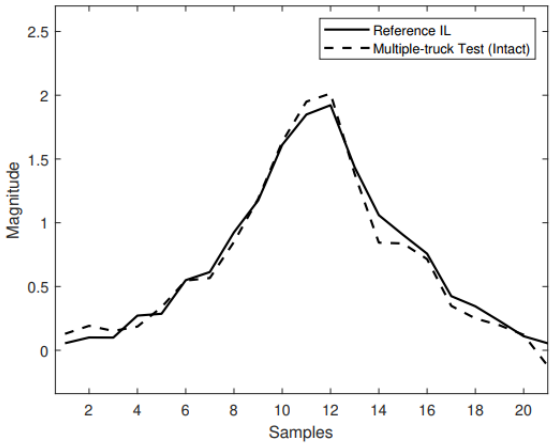

(b) Reference IL2 vs. the IL of a multiple-truck event (Two 5-axletrucks).

Figure 0.1. Reference IL vs. IL of the intact bridge subjected to test trucks.

Table 0.1. Thresholds and the DI values for different trucks on the intact bridge in different transverse positions and with different noise contents.

Truck Type	Event Type	Transverse Position 1			Transverse Position 2			Transverse Position 3			Threshold
		NC1[a]	NC2	NC3	NC1	NC2	NC3	NC1	NC2	NC3	(UL[b])
3-axle	Single	0.066	0.084	0.073	0.020	0.016	0.023	0.038	0.071	0.049	0.066
4-axle		0.044	0.056	0.050	0.018	0.009	0.013	0.034	0.038	0.050	0.046
5-axle		0.042	0.045	0.060	0.039	0.026	0.019	0.046	0.031	0.039	0.047
3-axle	Mult.	0.130	0.115	0.163	0.229	0.195	0.199	0.307	0.389	0.315	0.287
4-axle		0.244	0.317	0.220	0.351	0.306	0.401	0.620	0.452	0.540	0.471
5-axle		0.210	0.286	0.288	0.271	0.269	0.220	0.176	0.296	0.193	0.275

[a]NC=Noise content, [b]UL=Upper limit with 95% confidence

5.2. Single-truck and multiple truck events

Once the reference ILs and the thresholds were obtained, eleven different damage scenarios shown in Figure 3.7 were tested to understand if the proposed dual-purpose SHM procedure can be used when any of the damage scenarios occur. Thus, each truck moved once for each damage scenario (a total of 11 for each truck and 33 for all trucks) in a single-truck event, and the new ILs as well as DI values were obtained. Figure 5.2 shows the DI values for each truck and each damage scenario. Colored elements in Figure 5.2 mean that the DI values are greater than the DI thresholds specified in Table 5.1. The purpose of using several trucks was to improve the bridge monitoring accuracy. In fact, the SHM outcome will be the summation of all covered elements for each truck type. However, Figure 5.2 shows that for single-truck events, only one truck could be enough to realize if any damage has occurred in the region of interest (shown in Figure 3.7). This is because, for all damage scenarios and truck types, the DI values were significantly greater than the thresholds. Figure 5.3 shows an example to reveal how the damaged IL looks like compared to the reference IL1 for damage scenario 2.

3-axle					4-axle					5-axle					Covered			
0.360	1.022	0.549	0.439	+	0.581	0.997	0.586	0.541	+	0.821	1.577	1.082	0.879	=	1	3	6	9
24.260	0.524	0.415	0.371		21.896	0.845	0.654	0.537		28.096	1.109	0.994	0.862		2	4	7	10
	2.200	0.978	0.517			2.500	1.231	0.712			2.705	1.577	0.956			5	8	11

Figure 0.2. The DI values for the damaged bridge under a single truck and the covered damage positions.

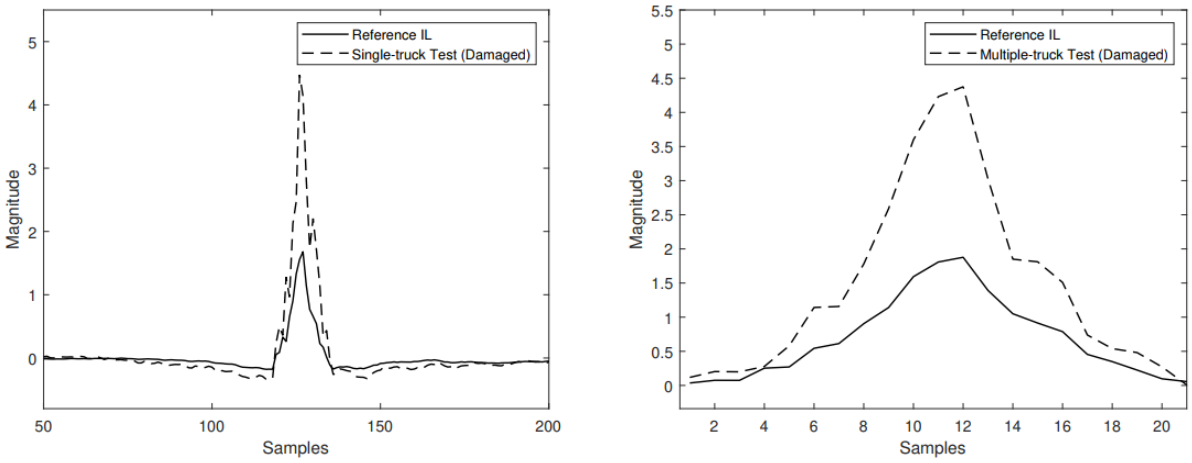

(a) Single 5-axle truck (DI=28.096) ***(b) Multiple 5-axle trucks (DI=24.640)***

Figure 0.3. The results of multiple-truck cases.

However, as mentioned in Chapter 2, sometimes, multiple trucks will be simultaneously on the bridge that should be handled with the new IL extraction technique (MP-IL). To evaluate the capability of the MP-IL technique, 33 multiple-truck analyses were conducted using each truck (i.e., two in-one-row 3-axle trucks, etc.) and for each damage scenario. The DI values are shown in Figure 5.4 for each multiple-truck event. According to Figure 5.4, damage scenarios 2, 3, 4, 5, 7, 8 are covered using all trucks. However, some other damage scenarios are only covered by a certain truck type (1, 6, 11), and some (9, 10) are not covered at all. Considering all truck types, only two damage scenarios are not covered. This shows that the dual-purpose procedure can work effectively even for multiple-truck events, and also, the idea of incorporating different types of trucks could improve the accuracy. This is further discussed later in chapter to realize why using different trucks can improve the results. Figure 5.3 shows an example to compare the damaged IL with the reference IL2 for damage scenario 2.

According to the results for single-truck and multiple-truck events, it can be concluded that the single-truck events can easier identify the damage, and only one truck can be enough. This is because, in the standard IL technique used for single-truck events, the entire strain will be used while MP-IL first removes the non-localized portion to decompose the strain responses associated with each truck. Thus, the single-truck events are more likely to generate a higher value than the threshold and capture the damage. However, the standard IL and MP-IL are complementary, and both are needed for the dual-purpose SHM procedure since it is not guaranteed to only have one truck on the bridge during the bridge monitoring process.

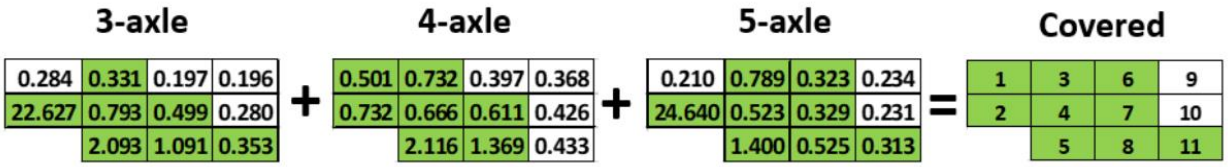

Figure 0.4. The DI values for the damaged bridge under multiple trucks and the covered damage positions.

Lastly, the instrumentation plan should be updated to effectively work for both BWIM and SHM to cover all damage scenarios for the damage intensity considered. It was mentioned in Chapter 3 that the initial distance between the successive sensors was selected to be 1.6m per previously published BWIM studies. It was observed that all damage scenarios were covered in single-truck and multiple-truck events except for scenarios 9 and 10 in the latter event. Thus, the successive distance between the sensors should be updated to 0.8 to 1 m (0.4-0.5 m from each sensor) for maximum effectiveness.

Now that it is shown the damage scenarios in the region of interest (shown in Figure 3.7) in the top-right quadrant can be effectively covered, it can be extended to other quadrants around each sensor, assuming a similar structural behavior in those regions. This assumption was made due to symmetry and to reduce the required analysis time since each analysis in CSI Bridge software takes 70 minutes. These results are the outcome of a minimum of 110 hours of effective analysis time.

5.3. Parametric study

It was already discussed about the variation made by noise and transverse position. This subsection discusses the effect of the truck characteristics on the DI values. When a different truck is used, three factors may change. These include the gross vehicle weight (GVW), axle weights' ratios, and axle spacings. To consider the effect of these factors, three cases (all 3-axles) with different characteristics (introduced in Table 3.4) were considered and compared with the original 3-axle truck as a reference (shown in Figure 3.8.a.

To ensure that other factors are necessarily constant, a new reference IL was computed for each truck using the strain response on the intact bridge. The same truck was then used on the damaged bridge with damage scenario 8. Also, noise and transverse positions were not included as well.

In Case 1, all trucks had the same axle weights' ratios and axle spacings, but their GVWs differed. According to the results shown in Figure 5.5, the DI values for Trucks 1 through 4 were all similar numbers ($0.576 < DI < 0.600$) compared to the original 3-axle truck (DI=0.599).

In Case 2, the second axle spacing changed from 4.5m to 6m (Truck 5) and 3m (Truck 6), while the GVWs and axle weights' ratios were constant. The DI variation was slightly higher than Case 1 (0.655 for Truck 5 and 0.535 for Truck 6).

In Case 3, only the axle weights' ratios changed, and the other two factors remained constant. According to the results, the DI values varied from 0.526 for Truck 7 to 0.646 for Truck 10.

Overall, it seems that the DI value range is in good agreement to the original DI related to the reference 3-axle truck. This shows that the IL extraction technique can successfully remove the effect of the truck characteristics and make it unique for a particular bridge, but still, some variations exist. This was already acknowledged by previously published studies in the BWIM area. For instance, this is clearly mentioned on the first page of the paper published on MLE method developed by Ieng in 2015 [39]. According to this study, the MLE method takes multiple trucks with multiple passages into account to include the variability of the effects of the calibration vehicles on the bridge. This was later agreed by other researchers in this area as well [40]. In fact, since IL computation takes the strain response and

produces the IL, the IL can slightly change from a truck to another truck with different characteristics, although it was shown that this variation is not significant. This could be due to a change in the strain response contents associated with different truck types. However, this variation was shown to be a positive factor for this study. In fact, it can be acceptable and even positive as long as we use separate reference ILs and DI thresholds for each truck (Table 5.1). This is a reasonable practice for a real-world application since, in SHM, we are able to use the same trucks for calibration and monitoring stages.

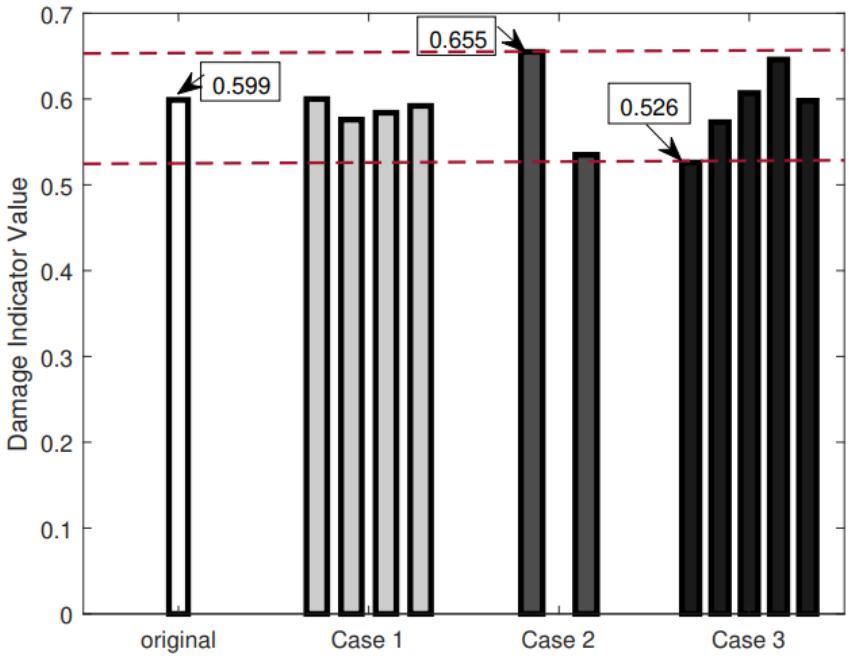

Figure 0.5. DI values for the cases specified in Table 3.4.

CHAPTER 6

Conclusions and future work

6.1. Phase I

The first phase reports the results of a study on a novel bridge-weigh-in-motion (BWIM) technique to estimate the traversing trucks' gross vehicle weights (GVW) and axle weights. This approach resolves the significant shortcoming of the existing BWIMs, which is their limitation for multiple simultaneous trucks on bridges. These may present with an arbitrary number of trucks and lightweight vehicles, simultaneously crossing the bridge in any traffic configuration. To show the applicability of the approach, a finite element model (validated against experimental data with great agreement) was used to consider single-truck events and complex multiple-truck traffic cases, including in-one-row trucks, zigzag patterns, side-by-side trucks, and a combination of several trucks with several lightweight vehicles. Based on the results, the following conclusions are made:

- When the sensors are placed where maximum localized strain occurs, the axles can be successfully captured even for closely-spaced ones.
- Removing the non-localized strain does not eliminate much important information when it is used for single-truck events. Compared to the standard BWIM approach, the proposed approach improved the GVW estimation from 4.1% error to 2.2% for lane one and from 4.8% to 2.4% for lane two. However, the mean absolute errors (MAE) of the axle weights were increased from 4.8% to 7.4% for lane one and from 6.5% to 10.6% for lane two. This increase in axle weight estimation still remains in a reasonable range, and simultaneously, the GVW estimation accuracy is improved, and multiple-truck weight estimation is enabled.
- The proposed approach was tested on two in-one-row trucks (a 5-axle and a 3-axle), two zigzag-pattern events (with three 3-axle trucks), a side-by-side case (with a 5-axle and 3-axle trucks), and a complex multiple-vehicle event with three trucks and two lightweight vehicles distributed in all three lanes. Results demonstrated that the proposed approach can successfully decompose the strain responses associated with each truck. Also, it can accurately estimate the GVWs and axle weights. The overall mean absolute errors, based on all complex multiple-truck cases, were respectively 4.5% and 11.3% for GVW and axle weight estimations. According to the results, out of fifteen trucks (in all six multiple-truck events), nine GVW errors were less than 5%, five errors were between 5% and 10%, and only one GVW error was greater than 10%. Additionally, out of 53 axle weight estimations, 44 cases had an error less than 20% (28 cases had an error less than 10% and 16 cases an error greater than 10% but less than 20%) and only 9 cases with an error greater than 20%. These results are comparable with expensive pavement-based WIM systems and traditional BWIM technologies.
- In this study, the fundamental goal was to present a proof-of-concept study to show that the proposed BWIM approach effectively works for single and multiple trucks with complex traffic patterns. Additionally, in an actual situation, it is usually very challenging to control the traffic (without lane closure) to consider desired/complex traffic load patterns with multiple trucks involved. Thus, a finite element model (validated against experimental data) was used to resolve this issue. However, in a future study, it is necessary to experimentally evaluate the proposed approach against a decent

number of multiple-truck events. Factors such as transverse position and temperature change should be carefully considered.

- Also, other than the techniques used in this study to remove the non-localized strain response (manual process, high-pass filter with low cut-off frequency, and envelope function), there might be other techniques which may improve the weight estimation results.

6.2. Phase II

In the second phase of this study, a dual-purpose structural health monitoring (SHM) approach is proposed to simultaneously monitor the integrity of multiple bridges (level I damage detection) using the BWIM system existing sensors. This procedure uses a novel multiple presence IL (MP-IL) technique for SHM application. Also, other factors such as noise and transverse position are also considered in the proposed procedure to provide a more realistic bridge health monitoring approach. The following conclusions were made:

- The noise and transverse position factors can make a maximum DI variation of 0.068 and 0.4 for the single-truck and multiple-truck events, respectively, showing a significant effect on the results.
- According to the results, damage scenarios 2, 3, 4, 5, 7, 8 were covered using all trucks. However, some other damage scenarios (e.g., 1, 6, 11) were only detected by a particular truck, and some (such as 9, 10) were not covered. However, only two damage scenarios were not detected considering all trucks together. This shows that the dual-purpose procedure can work effectively even for multiple-truck events. Also, the idea of incorporating different types of trucks could improve the accuracy.
- According to the results for single-truck and multiple-truck events, it can be concluded that the single-truck events can easier identify the damage, and only one truck can be enough. This is because, in the standard IL technique used for single-truck events, the entire strain will be used while MP-IL first removes the non-localized portion to decompose the strain responses associated with each truck. Thus, the single-truck events are more likely to generate a higher value than the threshold and capture the damage. However, the standard IL and MP-IL are complementary, and both are needed for the dual-purpose SHM procedure since it is not guaranteed to only have one truck on the bridge during the bridge monitoring process.
- An updated instrumentation plan that effectively work for both BWIM and SHM was proposed. It was shown that all damage scenarios were covered in single-truck and multiple-truck events except for scenarios 9 and 10 in the latter event. Thus, in the updated instrumentation plan, the successive distance between the sensors was decreased to 0.8 to 1 m for a maximum effectiveness.
- Several cases were considered to consider the effect of the truck type. In Case 1, all trucks had the same axle weights' ratios and axle spacings, but their GVWs changed. the DI values for Trucks 1 through 4 were all similar numbers ($0.576 < DI < 0.600$) compared to the original 3-axle truck with a DI value of 0.599. In Case 2, the second axle spacing changed and the axle weights' ratios and GVWs were constant. The DI variation was slightly higher than Case 1 (0.655 for Truck 5 and 0.535 for Truck 6). In Case 3, only the axle weights' ratios changed, and the other two factors remained constant. According to the results, the DI values differed from 0.526 for Truck 7 to 0.646 for Truck 10. However, it was concluded that the DI values were in good agreement to the DI value of the reference truck. This slight variation was shown to be a positive factor for SHM application, as long as separate reference ILs and DI thresholds are used for each truck. This makes it a reasonable practice for a real-world application since one is able to use the same trucks for both calibration and monitoring stages.
- In this study, it was aimed to prove the capability of the novel BWIM system for both weight estimation and SHM applications in multiple-presence events. However, it is necessary to experimentally evaluate the proposed dual-purpose SHM approach in a future study. Factors such as transverse position, noise, and temperature change should be also considered properly.

References

[1] C. Wang, H. Zhang, and Q. Li, "Reliability assessment of aging structures subjected to gradual and shock deteriorations," Reliab. Eng. Syst. Saf., vol. 161, pp. 78–86, May 2017, doi: 10.1016/j.ress.2017.01.014.

[2] B. Heitner, F. Schoefs, E. J. OBrien, A. Žnidarič, and T. Yalamas, "Using the unit influence line of a bridge to track changes in its condition," J. Civ. Struct. Health Monit., vol. 10, no. 4, pp. 667–678, Sep. 2020, doi: 10.1007/s13349-020-00410-7.

[3] W. Han, J. Wu, C. S. Cai, and S. Chen, "Characteristics and Dynamic Impact of Overloaded Extra Heavy Trucks on Typical Highway Bridges," J. Bridge Eng., vol. 20, no. 2, p. 05014011, Feb. 2015, doi: 10.1061/(ASCE)BE.1943-5592.0000666.

[4] F. Huseynov, C. Kim, E. J. OBrien, J. M. W. Brownjohn, D. Hester, and K. C. Chang, "Bridge damage detection using rotation measurements – Experimental validation," Mech. Syst. Signal Process., vol. 135, p. 106380, Jan. 2020, doi: 10.1016/j.ymssp.2019.106380.

[5] S. M. Khan, S. Atamturktur, M. Chowdhury, and M. Rahman, "Integration of Structural Health Monitoring and Intelligent Transportation Systems for Bridge Condition Assessment: Current Status and Future Direction," IEEE Trans. Intell. Transp. Syst., vol. 17, no. 8, pp. 2107–2122, Aug. 2016, doi: 10.1109/TITS.2016.2520499.

[6] B. Jacob and V. Feypell-de La Beaumelle, "Improving truck safety: Potential of weigh-in-motion technology," IATSS Res., vol. 34, no. 1, pp. 9–15, Jul. 2010, doi: 10.1016/j.iatssr.2010.06.003.

[7] P. Burnos and J. Gajda, "Thermal Property Analysis of Axle Load Sensors for Weighing Vehicles in Weigh-in-Motion System," Sensors, vol. 16, no. 12, Art. no. 12, Dec. 2016, doi: 10.3390/s16122143.

[8] A. González, A. T. Papagiannakis, and E. J. O'Brien, "Evaluation of an Artificial Neural Network Technique Applied to Multiple-Sensor Weigh-in-Motion Systems," Transp. Res. Rec., vol. 1855, no. 1, pp. 151–159, Jan. 2003, doi: 10.3141/1855-19.

[9] J. Wang and M. Wu, "An overview of research on weigh-in-motion system," in Fifth World Congress on Intelligent Control and Automation (IEEE Cat. No.04EX788), Jun. 2004, vol. 6, pp. 5241-5244 Vol.6. doi: 10.1109/WCICA.2004.1343721.

[10] Y. Yu, C. Cai, and L. Deng, "State-of-the-art review on bridge weigh-in-motion technology," Adv. Struct. Eng., vol. 19, no. 9, pp. 1514–1530, Sep. 2016, doi: 10.1177/1369433216655922.

[11] F. Moses, "Weigh-in-Motion System Using Instrumented Bridges," Transp. Eng. J. ASCE, vol. 105, no. 3, pp. 233–249, May 1979, doi: 10.1061/TPEJAN.0000783.

[12] M. Lydon, S. E. Taylor, D. Robinson, A. Mufti, and E. J. O. Brien, "Recent developments in bridge weigh in motion (B-WIM)," J. Civ. Struct. Health Monit., vol. 6, no. 1, pp. 69–81, Feb. 2016, doi: 10.1007/s13349-015-0119-6.

[13] T. Ojio, C. H. Carey, E. J. OBrien, C. Doherty, and S. E. Taylor, "Contactless Bridge Weigh-in-Motion," J. Bridge Eng., vol. 21, no. 7, p. 04016032, Jul. 2016, doi: 10.1061/(ASCE)BE.1943-5592.0000776.

[14] J. Lee, K.-C. Lee, S. Jeong, Y.-J. Lee, and S.-H. Sim, "Long-term displacement measurement of full-scale bridges using camera ego-motion compensation," Mech. Syst. Signal Process., vol. 140, p. 106651, Jun. 2020, doi: 10.1016/j.ymssp.2020.106651.

[15] T. Bao, S. K. Babanajad, T. Taylor, and F. Ansari, "Generalized Method and Monitoring Technique for Shear-Strain-Based Bridge Weigh-in-Motion," J. Bridge Eng., vol. 21, no. 1, p. 04015029, Jan. 2016, doi: 10.1061/(ASCE)BE.1943-5592.0000782.

[16] E. O'Brien, D. Hajializadeh, N. Uddin, D. Robinson, and R. Opitz, "Strategies for axle detection in bridge weigh-in-motion systems," in Proceedings of the International Conference on Weigh-in-Motion (ICWIM 6), 2012, pp. 79–88.

[17]M. Lydon, D. Robinson, S. E. Taylor, G. Amato, E. J. O. Brien, and N. Uddin, "Improved axle detection for bridge weigh-in-motion systems using fiber optic sensors," J. Civ. Struct. Health Monit., vol. 7, no. 3, pp. 325–332, Jul. 2017, doi: 10.1007/s13349-017-0229-4.
[18]H. Kalhori, M. M. Alamdari, X. Zhu, B. Samali, and S. Mustapha, "Non-intrusive schemes for speed and axle identification in bridge-weigh-in-motion systems," Meas. Sci. Technol., vol. 28, no. 2, p. 025102, Jan. 2017, doi: 10.1088/1361-6501/aa52ec.
[19]E. J. O'Brien, A. Znidaric, W. Baumgärtner, A. González, and P. McNulty, Weighing-In-Motion of Axles and Vehicles for Europe (WAVE) WP1. 2: Bridge WIM Systems. University College Dublin, 2001.
[20]T. Bao, S. K. Babanajad, T. Taylor, and F. Ansari, "Generalized Method and Monitoring Technique for Shear-Strain-Based Bridge Weigh-in-Motion," J. Bridge Eng., vol. 21, no. 1, p. 04015029, Jan. 2016, doi: 10.1061/(ASCE)BE.1943-5592.0000782.
[21]J. Kalin, A. Žnidarič, I. Lavrič, and B. Sc, "Practical implementation of nothing-on-the-road bridge weigh-in-motion system," 2006.
[22]W. He, L. Deng, H. Shi, C. S. Cai, and Y. Yu, "Novel Virtual Simply Supported Beam Method for Detecting the Speed and Axles of Moving Vehicles on Bridges," J. Bridge Eng., vol. 22, no. 4, p. 04016141, Apr. 2017, doi: 10.1061/(ASCE)BE.1943-5592.0001019.
[23]Y. Yu, C. Cai, and L. Deng, "Vehicle axle identification using wavelet analysis of bridge global responses," J. Vib. Control, vol. 23, no. 17, pp. 2830–2840, Oct. 2017, doi: 10.1177/1077546315623147.
[24]L. Deng, W. He, Y. Yu, and C. S. Cai, "Equivalent Shear Force Method for Detecting the Speed and Axles of Moving Vehicles on Bridges," J. Bridge Eng., vol. 23, no. 8, p. 04018057, Aug. 2018, doi: 10.1061/(ASCE)BE.1943-5592.0001278.
[25]W. He, T. Ling, E. J. OBrien, and L. Deng, "Virtual Axle Method for Bridge Weigh-in-Motion Systems Requiring No Axle Detector," J. Bridge Eng., vol. 24, no. 9, p. 04019086, Sep. 2019, doi: 10.1061/(ASCE)BE.1943-5592.0001474.
[26]D. Cantero, R. Karoumi, and A. González, "The Virtual Axle concept for detection of localised damage using Bridge Weigh-in-Motion data," Eng. Struct., vol. 89, pp. 26–36, Apr. 2015, doi: 10.1016/j.engstruct.2015.02.001.
[27]H. Wang, T. Nagayama, B. Zhao, and D. Su, "Identification of moving vehicle parameters using bridge responses and estimated bridge pavement roughness," Eng. Struct., vol. 153, pp. 57–70, Dec. 2017, doi: 10.1016/j.engstruct.2017.10.006.
[28]Y. Wang and W.-L. Qu, "Moving train loads identification on a continuous steel truss girder by using dynamic displacement influence line method," Int. J. Steel Struct., vol. 11, no. 2, pp. 109–115, Jun. 2011, doi: 10.1007/s13296-011-2001-7.
[29]J. Dowling, E. J. OBrien, and A. González, "Adaptation of Cross Entropy optimisation to a dynamic Bridge WIM calibration problem," Eng. Struct., vol. 44, pp. 13–22, Nov. 2012, doi: 10.1016/j.engstruct.2012.05.047.
[30]N.-B. Wang, L.-X. He, W.-X. Ren, and T.-L. Huang, "Extraction of influence line through a fitting method from bridge dynamic response induced by a passing vehicle," Eng. Struct., vol. 151, pp. 648–664, Nov. 2017, doi: 10.1016/j.engstruct.2017.06.067.
[31]E. J. OBrien, M. J. Quilligan, and R. Karoumi, "Calculating an influence line from direct measurements," Proc. Inst. Civ. Eng. - Bridge Eng., vol. 159, no. 1, pp. 31–34, Mar. 2006, doi: 10.1680/bren.2006.159.1.31.
[32]E. J. OBrien, C. W. Rowley, A. Gonzalez, and M. F. Green, "A regularised solution to the bridge weigh-in-motion equations," Int. J. Heavy Veh. Syst., vol. 16, no. 3, pp. 310–327, Jan. 2009, doi: 10.1504/IJHVS.2009.027135.
[33]E. J. OBrien, L. Zhang, H. Zhao, and D. Hajializadeh, "Probabilistic bridge weigh-in-motion," Can. J. Civ. Eng., vol. 45, no. 8, pp. 667–675, Aug. 2018, doi: 10.1139/cjce-2017-0508.
[34]H. Zhao, N. Uddin, E. J. O'Brien, X. Shao, and P. Zhu, "Identification of Vehicular Axle Weights with a Bridge Weigh-in-Motion System Considering Transverse Distribution of Wheel Loads," J. Bridge Eng., vol. 19, no. 3, p. 04013008, Mar. 2014, doi: 10.1061/(ASCE)BE.1943-5592.0000533.
[35]J. Richardson, S. Jones, A. Brown, E. O'Brien, and D. Hajializadeh, "On the use of bridge weigh-in-motion for overweight truck enforcement," Int. J. Heavy Veh. Syst., vol. 21, no. 2, pp. 83–104, Jan. 2014, doi: 10.1504/IJHVS.2014.061632.
[36]X. Zheng, D.-H. Yang, T.-H. Yi, and H.-N. Li, "Development of bridge influence line identification methods based on direct measurement data: A comprehensive review and comparison," Eng. Struct., vol. 198, p. 109539, Nov. 2019, doi: 10.1016/j.engstruct.2019.109539.

[37]E. J. OBrien, M. J. Quilligan, and R. Karoumi, "Calculating an influence line from direct measurements," Proc. Inst. Civ. Eng. - Bridge Eng., vol. 159, no. 1, pp. 31–34, Mar. 2006, doi: 10.1680/bren.2006.159.1.31.
[38]E. J. OBrien, C. W. Rowley, A. Gonzalez, and M. F. Green, "A regularised solution to the bridge weigh-in-motion equations," Int. J. Heavy Veh. Syst., vol. 16, no. 3, pp. 310–327, Jan. 2009, doi: 10.1504/IJHVS.2009.027135.
[39]S.-S. Ieng, "Bridge Influence Line Estimation for Bridge Weigh-in-Motion System," J. Comput. Civ. Eng., vol. 29, no. 1, p. 06014006, Jan. 2015, doi: 10.1061/(ASCE)CP.1943-5487.0000384.
[40]F. Carraro, M. S. Gonçalves, R. H. Lopez, L. F. F. Miguel, and A. M. Valente, "Weight estimation on static B-WIM algorithms: A comparative study," Eng. Struct., vol. 198, p. 109463, Nov. 2019, doi: 10.1016/j.engstruct.2019.109463.
[41]H. Kalhori, M. Makki Alamdari, X. Zhu, and B. Samali, "Nothing-on-Road Axle Detection Strategies in Bridge-Weigh-in-Motion for a Cable-Stayed Bridge: Case Study," J. Bridge Eng., vol. 23, no. 8, p. 05018006, Aug. 2018, doi: 10.1061/(ASCE)BE.1943-5592.0001259.
[42]D. Dounsuvanh, P. Pheinsusom, and Y. Sato, "THAI TRUCK LOADING MONITORING USING BWIM SYSTEM," ASEAN Eng. J., vol. 3, no. 2, Art. no. 2, 2014, doi: 10.11113/aej.v3.15525.
[43]F. C. MS, A. VALENTE, R. LOPEZ, L. MIGUEL, and R. PINTO, "EFFECTIVENESS OF THE CORRELATION APPROACH FOR DETERMINATION OF VEHICLE VELOCITY ON REAL WORLD NOR-BWIM DATA," ICWIM8, p. 61, 2019.
[44]M. Quilligan, R. Karoumi, and E. J. O'Brien, "Development and testing of a 2-dimensional multi-vehicle bridge-WIM algorithm," in 3rd International Conference on Weigh-in-Motion (ICWIM3), 2002, pp. 199–208.
[45]S.-Z. Chen, G. Wu, and D.-C. Feng, "Development of a bridge weigh-in-motion method considering the presence of multiple vehicles," Eng. Struct., vol. 191, pp. 724–739, Jul. 2019, doi: 10.1016/j.engstruct.2019.04.095.
[46]Y. Yu, C. S. Cai, and L. Deng, "Nothing-on-road bridge weigh-in-motion considering the transverse position of the vehicle," Struct. Infrastruct. Eng., vol. 14, no. 8, pp. 1108–1122, Aug. 2018, doi: 10.1080/15732479.2017.1401095.
[47]N. Zolghadri, M. W. Halling, N. Johnson, and P. J. Barr, "Field Verification of Simplified Bridge Weigh-in-Motion Techniques," J. Bridge Eng., vol. 21, no. 10, p. 04016063, Oct. 2016, doi: 10.1061/(ASCE)BE.1943-5592.0000930.
[48]A. Žnidarič, I. Lavrič, J. Kalin, and M. Kreslin, "Using strips to mitigate the multiple-presence problem of BWIM systems," 2012.
[49]Z.-W. Chen, S. Zhu, Y.-L. Xu, Q. Li, and Q.-L. Cai, "Damage Detection in Long Suspension Bridges Using Stress Influence Lines," J. Bridge Eng., vol. 20, no. 3, p. 05014013, Mar. 2015, doi: 10.1061/(ASCE)BE.1943-5592.0000681.
[50]R. Sarlo, P. A. Tarazaga, and M. E. Kasarda, "High resolution operational modal analysis on a five-story smart building under wind and human induced excitation," Eng. Struct., vol. 176, pp. 279–292, Dec. 2018, doi: 10.1016/j.engstruct.2018.08.060.
[51]M. H. SoleimaniBabakamali, A. Moghadam, R. Sarlo, M. H. Hebdon, and P. S. Harvey, "Mast Arm Monitoring via Traffic Camera Footage: A Pixel-Based Modal Analysis Approach," Exp. Tech., vol. 45, no. 3, pp. 329–343, Jun. 2021, doi: 10.1007/s40799-020-00422-4.
[52]W. Heylen, S. Lammens, and P. Sas, "Modal Analysis Theory and Testing, Dept. of Mech," Engrg Kathol. Univ Leuven Heverlee Belg., 1995.
[53]N. M. M. Maia, J. M. M. Silva, E. A. M. Almas, and R. P. C. Sampaio, "DAMAGE DETECTION IN STRUCTURES: FROM MODE SHAPE TO FREQUENCY RESPONSE FUNCTION METHODS," Mech. Syst. Signal Process., vol. 17, no. 3, pp. 489–498, May 2003, doi: 10.1006/mssp.2002.1506.
[54]Z. Y. Shi, S. S. Law, and L. M. Zhang, "STRUCTURAL DAMAGE LOCALIZATION FROM MODAL STRAIN ENERGY CHANGE," J. Sound Vib., vol. 218, no. 5, pp. 825–844, Dec. 1998, doi: 10.1006/jsvi.1998.1878.
[55]T.-J. Huang, Z. Liang, and G. C. Lee, "Structural damage detection using energy transfer ratios(ETR)," in International Modal Analysis Conference(IMAC), 14 th, Dearborn, MI, 1996, pp. 126–132.
[56]M. Breccolotti and M. Natalicchi, "Bridge Damage Detection Through Combined Quasi-static Influence Lines and Weigh-in-motion Devices," Int. J. Civ. Eng., vol. 20, no. 5, pp. 487–500, May 2022, doi: 10.1007/s40999-021-00682-0.

[57]Y. Zeinali and B. A. Story, "Impairment localization and quantification using noisy static deformation influence lines and Iterative Multi-parameter Tikhonov Regularization," Mech. Syst. Signal Process., vol. 109, pp. 399–419, Sep. 2018, doi: 10.1016/j.ymssp.2018.02.036.
[58]S. Zhang and Y. Liu, "Damage Detection in Beam Bridges Using Quasi-static Displacement Influence Lines," Appl. Sci., vol. 9, no. 9, Art. no. 9, Jan. 2019, doi: 10.3390/app9091805.
[59]M. M. Alamdari, K. Kildashti, B. Samali, and H. V. Goudarzi, "Damage diagnosis in bridge structures using rotation influence line: Validation on a cable-stayed bridge," Eng. Struct., vol. 185, pp. 1–14, Apr. 2019, doi: 10.1016/j.engstruct.2019.01.124.
[60]D. Cantero and A. González, "Bridge damage detection using weigh-in-motion technology," J. Bridge Eng., vol. 20, no. 5, p. 04014078, 2015.
[61]C. R. Johnson Jr, W. A. Sethares, and A. G. Klein, Software receiver design: build your own digital communication system in five easy steps. Cambridge University Press, 2011.
[62]A. Moghadam, M. AlHamaydeh, and R. Sarlo, "Bridge-weigh-in-motion approach for simultaneous multiple vehicles on concrete-box-girder bridges," Autom. Constr., vol. 137, p. 104179, May 2022, doi: 10.1016/j.autcon.2022.104179.
[63]M. D. Fontaine, L. E. Dougald, and C. S. Bhamidipati, "Evaluation of Truck Lane Restrictions in Virginia: Phase II," Virginia Transportation Research Council, 2009.
[64]R. Berard and A. Bourion, "Truck widths and paths," Transp. Res. Circ., no. E-C003, p. 14:1–9, 1998.
[65]R. O. DECISION, "Federal Highway Administration," US Dep. OfTransportation Wash. DC, 2015.